Progress in Polymer Science 37 (2012) 1401–1424

Contents lists available at SciVerse ScienceDirect

Progress in Polymer Science

journal homepage: www.elsevier.com/locate/ppolysci

Evolution of polymeric hollow fibers as sustainable technologies: Past, present, and future

Na Peng[a], Natalia Widjojo[a], Panu Sukitpaneenit[a], May May Teoh[a], G. Glenn Lipscomb[b], Tai-Shung Chung[a,*], Juin-Yih Lai[c,**]

[a] Department of Chemical & Biomolecular Engineering, National University of Singapore, 4 Engineering Drive 4, Singapore 117576, Singapore
[b] Chemical and Environmental Engineering (MS 305), University of Toledo, 2801 West Bancroft Street, Toledo, OH 43606-3390, USA
[c] R&D Center for Membrane Technology, Department of Chemical Engineering, Chung Yuan Christian University, Taoyuan 320, Taiwan

ARTICLE INFO

Article history:
Received 28 March 2011
Received in revised form 17 January 2012
Accepted 23 January 2012
Available online 30 January 2012

Keywords:
Polymeric membrane
Hollow fiber
Membrane formation
Spinning
Phase inversion

ABSTRACT

Energy, water, affordable healthcare and global warming are four major global concerns resulting from resource depletion, record high oil prices, clean water shortages, high costs of pharmaceuticals, and changing climate conditions. Among many potential solutions, advances in membrane technology afford direct, effective and feasible approaches to solve these sophisticated issues. Membrane technology encompasses numerous technology areas including materials science and engineering, chemistry and chemical engineering, separation and purification phenomena, molecular simulation, as well as process and product design. Currently, polymeric hollow fiber membranes made using a non-solvent-induced phase inversion process are the dominant products because polymers offer a broad spectrum of materials chemistry and result in membranes with desirable physicochemical properties for diverse applications. Their low cost and ease of fabrication make polymeric membranes superior to inorganic membranes. Therefore, this review focuses on state-of-the-art polymeric hollow fiber membranes made from non-solvent-induced phase inversion and the potential of membrane processes for sustainable water and energy production. The specific topics include: (i) basic principles of hollow fiber membrane formation and the phase inversion process; (ii) membranes for energy (natural gas, H_2, and biofuel) production; (iii) membranes for CO_2 capture; and (iv) emerging desalination technologies (forward osmosis and membrane distillation) for water production. Finally, future opportunities and challenges for the development of advanced membrane structures are discussed.

© 2012 Elsevier Ltd. All rights reserved.

Contents

* Corresponding author. Fax: +65 6779 1936.
** Corresponding author. Fax: +886 3 2654198.
E-mail addresses: chencts@nus.edu.sg (T.-S. Chung), jylai@cycu.edu.tw (J.-Y. Lai).

0079-6700/$ – see front matter © 2012 Elsevier Ltd. All rights reserved.
doi:10.1016/j.progpolymsci.2012.01.001

1. Introduction

Since Loeb and Sourirajan [1] invented asymmetric cellulose acetate reverse osmosis (RO) membranes via phase inversion in the late 1950s, membranes with different materials and designs have been progressively developed for diverse applications in reverse osmosis (RO), micro/nano/ultra-filtration (MF,NF,UF), dialysis, gas separation, and pervaporation. At present, there are many types of membrane configurations available in the market, such as flat sheet composite membranes, polymeric hollow fibers, and inorganic tubular membranes. Hollow fiber membranes made of polymeric materials, first patented by Mahon [2] five decades ago, are highly competitive with flat and inorganic membranes because they possess several beneficial features. Compared to other membrane configurations, the hollow fiber geometry offers a larger effective membrane area per unit volume of the separation device (i.e., membrane module) which results in greater process intensification. Additionally, the hollow fiber form provides good self mechanical support and ease of handling during module fabrication and process operation.

A rich literature on membrane formation mechanisms and applications of hollow fiber membranes has been established during the past five decades [2–12]. Most efforts focused on innovative approaches for the formation of hollow fibers with an ultra-thin selective layer and physicochemical properties that improve dramatically separation performance. The membrane community has tried to adopt casting conditions used for flat-sheet membranes to spin comparable hollow fiber membranes. However, the formation mechanism for hollow fiber membranes via phase inversion is considerably more complex than that for flat-sheet membranes, and the factors controlling hollow fiber structure are distinctly different from those for flat sheets. One essential difference is the dope formulation: a sufficiently high polymer dope concentration is required for hollow fiber spinning. This usually results in much more complicated phase inversion properties and non-Newtonian rheological behavior. Moreover, in flat-sheet membrane formation, the phase inversion usually starts from the top surface of the as-cast film upon immersion in a coagulation bath, whereas hollow fiber fabrication involves two coagulants (internal and external coagulants). The internal coagulant controls the inner skin morphology, while the external coagulant controls the outer skin morphology. Other factors such as spinneret design, rheology within the spinneret, air-gap distance, moisture, die swell and elongational stresses also can impact final membrane morphology and performance.

The majority of the innovations and developments in hollow fiber membrane manufacture have been made through trial and error aided by past experience, empirical data, and qualitative scientific understanding. The potential for membrane technology to provide sustainable solutions to global demand for clean energy, water and health care has spurred membrane research and development to identify new polymeric materials with desirable properties and the advanced manufacturing technologies required to transform them into membranes. To transform these new materials into useful hollow fiber membranes and fully utilize their separation potential, researchers must understand the intrinsic physicochemical properties of these new materials, manipulate phase inversion processes, and control dope rheological responses during membrane formation to produce the desired membrane macro- and micro-structure.

Fabrication of hollow fiber membranes with both desirable morphology and separation performance is challenging. Macrovoids and irregular shapes are often observed in hollow fibers and they are considered as defects because they could lead to membrane mechanical failure if the membrane is operated under high pressure or subject to vibration for extended periods of time. Changes in polymer molecular structure to improve separation performance are limited by the well-known trade-off between permeability and selectivity—an increase in permeability usually is accompanied by a decrease in selectivity and vice

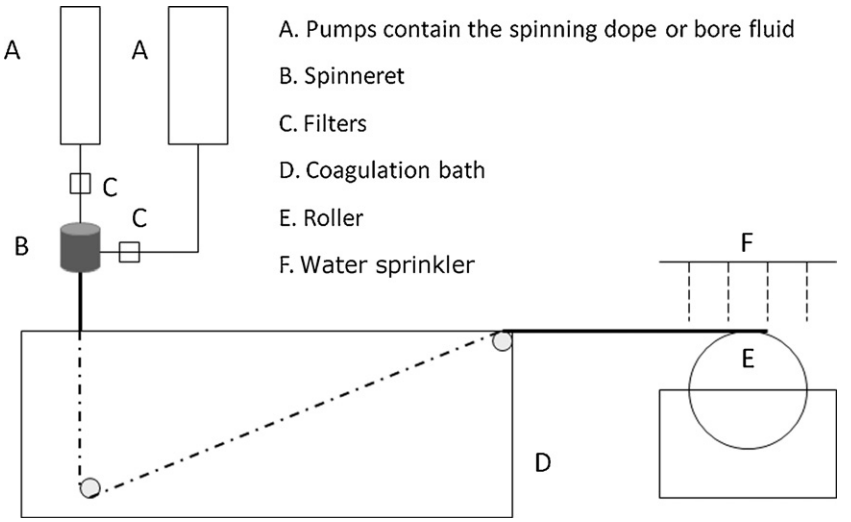

Fig. 1. Schematic diagram of hollow fiber spinning line.

versa. Even though many hollow fiber technologies have improved progressively during the last five decades, no comprehensive state-of-the-art review has been reported. Therefore, the objectives of this article are to: (1) review the efforts of membrane scientists to develop hollow fiber technologies with desirable membrane properties during the past 50 years; (2) review the state-of-the-art for polymeric hollow fiber formation especially in sustainability applications; and (3) provide perspectives for future hollow fiber membrane development.

2. Fundamentals of hollow fiber formation

2.1. Key elements and factors in hollow fiber spinning

Although a number of commercial hollow fiber membrane products are used industrially, three key elements determine their potential and application: (1) the pore size and pore-size distribution of the functional separation or selective layer, (2) the chemistry, mechanical and physicochemical properties of the membrane material; and (3) the thickness of the functional separation or selective layer and its substructure morphology. Among these three elements, proper selection of a membrane material is the most critical decision for production of high-performance hollow fiber membranes. Material chemistry and physics determine (1) the spinnability and mechanical strengths, (2) the inherent hydrophilicity/hydrophobicity and fouling tendency for water reuse, desalination and protein separation, (3) bio-compatibility for medical uses, and (4) chemical resistance and stability for applications in harsh environments. Once a potential material with an appropriate combination of mechanical and physicochemical properties is selected, membrane scientists must ingeniously design the hollow fiber membrane via phase inversion to ensure that it has desirable pore size, narrow pore-size distribution, ultrathin selective layer and open-cell sponge-like substructure morphology to maximize separation performance.

Commercially available polymeric hollow fiber membranes are usually spun from a hot spinneret with a short air-gap distance and a moderately high take-up speed. Fig. 1 illustrates a typical hollow fiber spinning line for the fabrication of polymeric hollow fibers via non-solvent-induced phase inversion and Fig. 2 shows an enlargement of the region near the spinneret. Once the dope solution is prepared and degassed, the hollow fiber spinning process usually consists of the following steps: (1) metering the spinning dope and bore fluid simultaneously by different precision pumps; (2) conveying the spinning solution

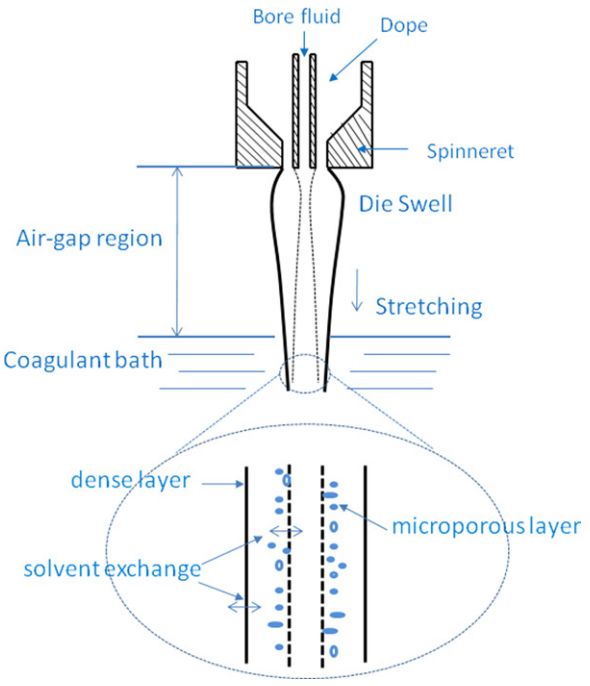

Fig. 2. Schematic diagram of area nearby the spinneret and the formation of nascent hollow fiber during phase inversion.

through a spinneret under shear and possibly converging flows; (3) internal coagulation when the bore fluid meets the dope exiting from the spinneret; (4) solvent evaporation from the outer nascent membrane surface in the air-gap region; (5) moisture-induced early phase separation in the outer nascent membrane surface in the air-gap region; (6) stretch by gravity and elongational forces induced by the take-up unit; (7) completion of phase inversion within the fiber wall and solidification induced by the external coagulation bath; and (8) solvent exchange or additional post-treatments to remove residual solvents and control pore size.

Before discussing the effects of spinning parameters on hollow fiber formation for a specific application, the key factors illustrated in Fig. 2 and their influence on membrane structure development are summarized. Solid concentration is an important parameter that plays a crucial role on overall fiber morphology and porosity. Usually, a higher solid concentration (often refers to polymer concentration) is required to form hollow fiber membranes for gas separation or pervaporation than those needed to form hollow fibers for water related separation applications such as ultrafiltration (UF) or microfiltration (MF). This observation arises from the fact that polymer solutions with a higher solid concentration usually have a higher viscosity and tend to induce chain entanglement, which can effectively reduce micro-defects and porosity in the membrane matrix.

During the precipitation of a nascent hollow fiber, the size (and associated diffusivity) of solvent molecules greatly determines the precipitation path and fiber morphology: a smaller, faster diffusing solvent molecule leads to faster solvent exchange, or vice versa. The coagulation rate also depends strongly on the solubility parameter difference between the dope solution and the coagulant: an increase in solubility parameter difference enhances the coagulation rate. Generally, a thick and relatively porous skin is formed if the coagulation rate is slow (which is referred as delayed demixing), while a thin but relatively dense layer is formed with fast coagulation (also referred to as instantaneous demixing). Since there are two coagulations taking place almost simultaneously in hollow fiber formation, membrane scientists can control the location and properties of the selective layer as well as the fiber cross-sectional morphology by properly adjusting solubility parameter differences between the dope solution and the inner/outer coagulants.

Most of the process parameters discussed thus far (e.g., dope viscosity, solubility parameter and coagulation rate) are a function of temperature. Therefore, the temperatures of the spinneret and coagulation bath can have a significant impact on fiber morphology. An increase in dope temperature leads to a reduction in dope viscosity while an increase in coagulation bath temperature leads to an increase in solvent exchange rate and solubility. Fig. 3 displays an example of the effect of various spinneret and coagulation bath temperatures on fiber morphology of Torlon® polyamideimide [13] and 6FDA/6FDAM polyimide membranes [14]. As the spinneret temperature increases, the viscosity of Torlon® solutions decreases and more macrovoids are formed on the fiber cross-section, while as the external coagulant temperature increases, a more porous structure is formed in 6FDA/6FDAM fibers because of delayed demixing.

The draw force induced by gravity due to the fiber's mass and the additional external draw force applied by the take-up unit can affect fiber surface structure and cross-section especially for large air-gaps and high take-up speeds. For example, the polyimide hollow fiber in Fig. 4(a) has a tight external surface morphology when wet-spun (no air-gap) but the dry-jet wet-spun fiber with a large air-gap has a three-dimensional open-cell structure [15]. This

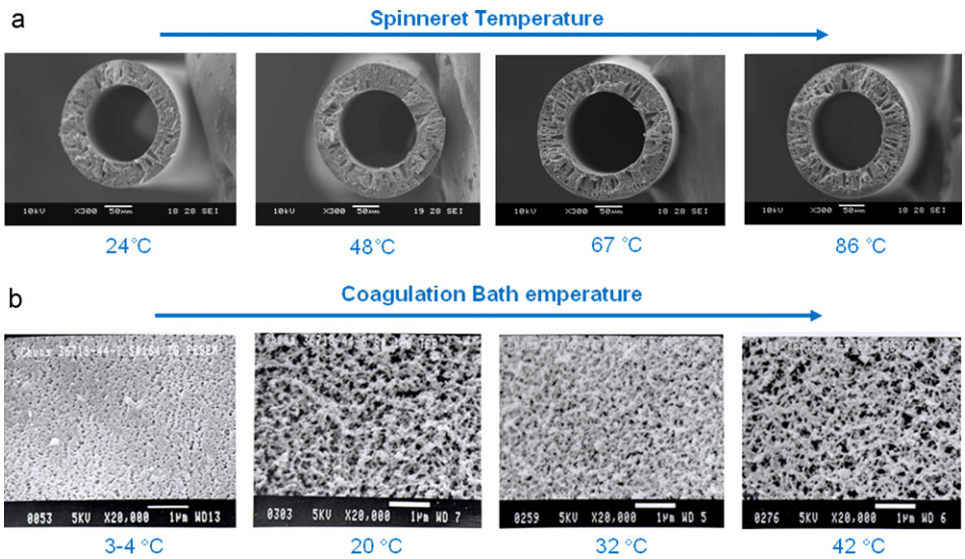

Fig. 3. The effect of spinning temperature on fiber morphology. (a) SEM cross-section images of Torlon® polyamideimide membranes spun at different spinneret temperatures [13] (Copyright 1997 John Wiley & Sons, Inc.). (b) SEM external surface images of 6FDA/6FDAM polyimide membranes spun at different coagulation bath temperatures [14]. (Copyright 2008, Elsevier B.V.)

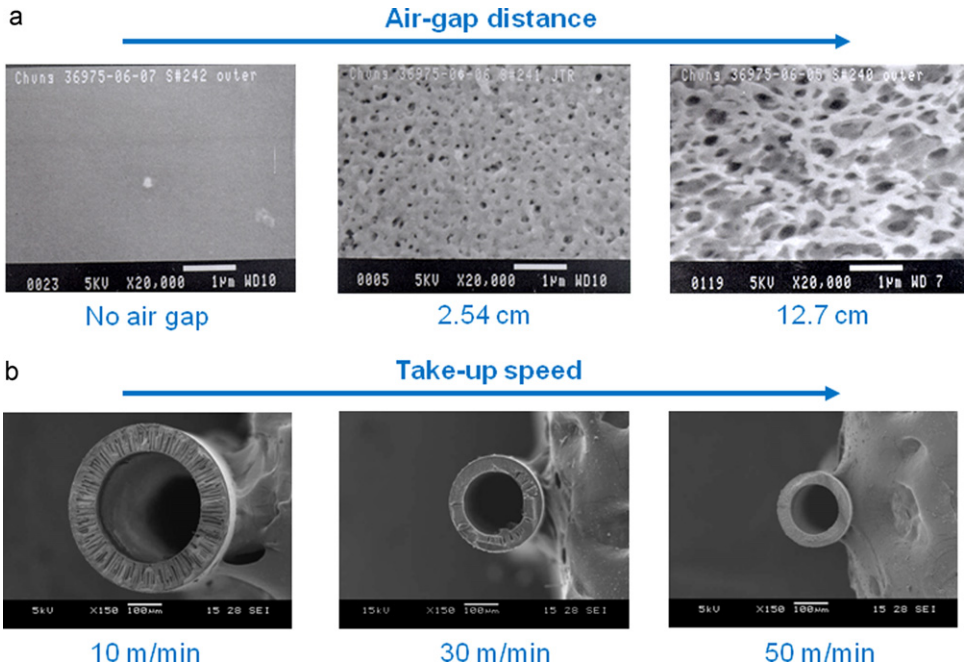

Fig. 4. The effect of air-gap distance and take-up speed on hollow fiber morphology. (a) SEM external surface images of 6FDA/6FDAM polyimide membranes with various air-gap lengths [15] (Copyright 1997, Elsevier Science B.V.), (b) SEM cross-section images of P84 polyimide membranes with various take-up speeds [16] (Copyright 2008, Elsevier B.V.).

phenomenon may arise from the different precipitation paths taken during the wet-spinning and dry-jet wet-spinning processes as well as elongation-induced chain orientation, packing and de-lamination. Fig. 4(b) demonstrates that macrovoid formation in a hollow fiber strongly depends on the take-up speed—sponge-like hollow fibers are produced in high speed spinning [16]. External elongational forces exerted by the take-up device also may affect the nascent hollow fiber by: (1) creating extra phase instability, (2) facilitating phase separation, and (3) inducing orientation and packing. The first two factors shorten the time for the solution to move from the binodal to the spinodal boundary or reduce the distance of the precipitation path between the two boundaries, while the last one results in an oriented polymer chain structure. However, reasonable values of the air-gap distance and take-up speed must be used in a spinning process. If the air-gap distance or take-up speed is too large, defects created by tearing chains apart may result from excessive elongational stresses.

2.2. *Phase inversion mechanisms during the membrane formation*

Before discussing technology developments for hollow fiber formation, the fundamentals of phase inversion are reviewed in this section. Phase inversion can be induced by non-solvent, vapor or temperature change. The introduction of non-solvents, so-called non-solvent-induced phase separation or immersion precipitation, is a widely used approach. During non-solvent-induced phase inversion, a homogeneous (thermodynamically stable) polymer solution is transformed into a polymer-rich phase (a high polymer concentration) and a polymer-lean phase (a high solvent concentration) to minimize the Gibbs free energy of mixing, ΔG_M, of the system [17]. For a simple ternary system consisting of a polymer, a solvent, and a non-solvent, ΔG_M at constant pressure and temperature can be calculated using the Flory–Huggins theory as follows:

$$\frac{\Delta G_m}{RT} = n_1 \ln\phi_1 + n_2 \ln\phi_2 + n_3 \ln\phi_3 + \chi_{12} n_1\phi_2 + \chi_{13} n_1\phi_3 + \chi_{23} n_2\phi_3, \quad (1)$$

where n_i, ϕ_1, and χ_i are the number of moles, volume fraction and binary interaction parameter, respectively. The polymer-rich phase predominately forms the membrane matrix, whereas the polymer-lean phase forms membrane pores. This phenomenon is typically regarded as liquid–liquid demixing.

The thermodynamic interactions between the three spinning dope components (polymer/solvent/non-solvent) and the concentration/phase changes that occur during phase inversion often are visualized using the ternary phase diagram first developed by Tompa in the late 1950s [18] and used by Strathmann et al. [19] and Michaels [20] in the early 1970s. Fig. 5 illustrates a typical ternary phase diagram where each corner of the triangle represents each pure component and any point located inside the triangle represents a mixture of the three components. The essential elements of a phase-diagram include the binodal and spinodal curves, critical point, tie-lines, and metastable region. The tie-line links two points on the binodal which are in thermodynamic equilibrium. One end-point of the tie-line represents the composition of polymer in the polymer-rich phase while the other end-point represents

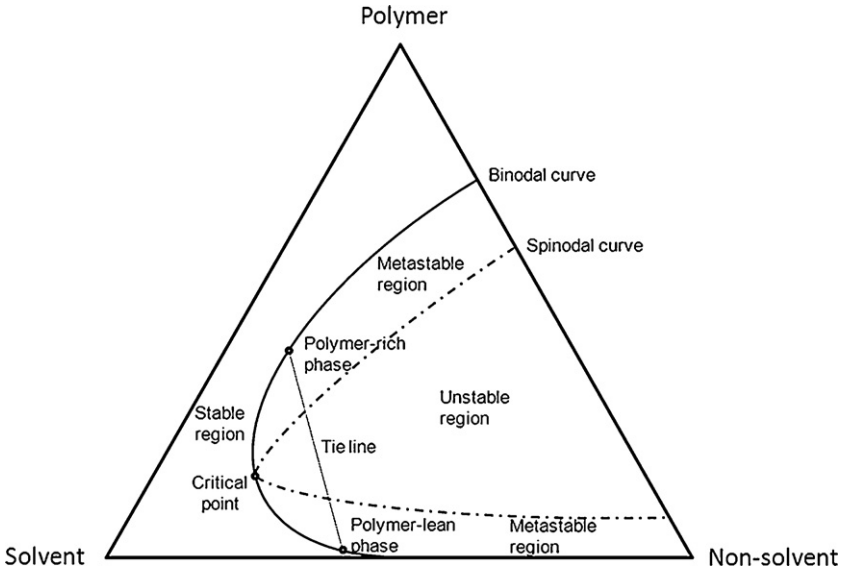

Fig. 5. Typical ternary phase diagram of a polymer–solvent–non-solvent system.

the composition of polymer in lean phase. The point of intersection between the binodal and spinodal curves is referred to as the critical point.

2.2.1. Phase inversion of glassy polymers

The thermodynamics of the system dictate whether liquid–liquid phase separation occurs by: (1) nucleation and growth or (2) spinodal decomposition [21]. Nucleation and growth occurs when the polymer solution moves from the thermodynamically stable region to the meta-stable region between the binodal and the spinodal curves in the phase diagram. Nucleation and growth of the polymer-rich phase in the lower (low polymer concentration) meta-stable region leads to polymer powders or low-integrity polymer agglomerates which are cannot be used as membranes. Conversely, nucleation and growth of the polymer-poor phase in the upper (high polymer concentration) meta-stable region results in a porous membrane morphology [6]. Phase separation by spinodal decomposition occurs when the system enters the thermodynamically unstable spinodal region directly by crossing the critical point or indirectly through the meta-stable region. Spinodal decomposition results from concentration fluctuations of increasing amplitude as opposed to nucleation and growth. Spinodal decomposition typically yields an "open-cell" or interconnected network structure, which is sometimes called a bicontinuous structure [21,22]. Most membrane scientists and engineers acknowledge that the morphological changes occurring during membrane formation by liquid–liquid demixing involve a combination of nucleation and growth and spinodal decomposition [15,18,23–25].

In practice, phase inversion is a dynamic process in which the polymer–solvent–non-solvent system changes composition rapidly due to fast multi-component mass transfer and diffusion-engendered convective flows. Thus, the kinetics of the process must be considered in addition to the equilibrium thermodynamics. For example, the ratio (referred to as the k value) of solvent outflow to non-solvent inflow plays a crucial role in controlling membrane structure and overall porosity [6,18,26–28] as illustrated in Fig. 6. Depending on the initial dope composition and the k value, the precipitation path may take place via the nucleation and growth or the spinodal decomposition mechanism. Since k may not be constant across the membrane thickness and its value is dependent on temperature and dope viscosity, prediction of the local membrane porosity is difficult. Therefore, Fig. 6 provides only a qualitative picture of the phase inversion process.

Many mass transfer models have been proposed to predict membrane formation during phase inversion [24–35]. Cohen et al. [35] and Reuvers et al. [24,25] are pioneers who proposed mass transfer models to explain membrane formation at the interface between the polymer solution and coagulation bath. Kim et al. [36] proposed a model of the spinodal decomposition mechanism based on the mass transfer that occurs during asymmetric membrane formation. Termonia [37] simulated polymer coagulation process using the Monte Carlo diffusion model. The model predicts membrane morphologies ranging from dust-like to finger-like and sponge-like by changing the interaction parameters between solvent and non-solvent coagulant. Termonia and co-workers recently reported that their model predicts the asymmetric structure can change from an island-like to a continuous phase in ultrafiltration membranes due to a shift in the phase separation mechanism from spinodal decomposition to nucleation and growth [38]. An attempt to investigate the effect of polymer chain length and solvent size on the kinetics of membrane formation during phase inversion using dynamic simulation was reported recently by Wang and co-workers [39].

The complexity of the phase inversion process increases dramatically if it involves solidification in addition to liquid–liquid demixing. Contradictory results are reported

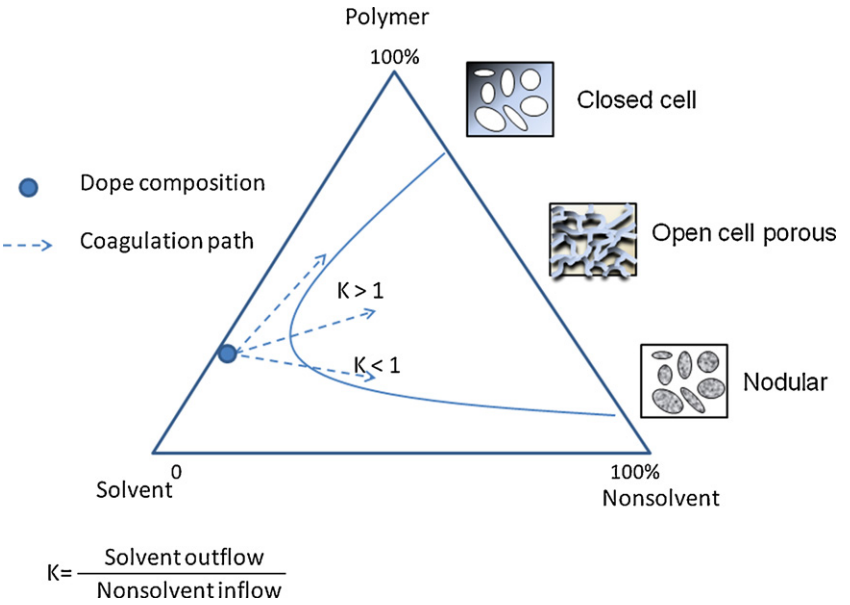

Fig. 6. Schematic diagram of the relationship of dope composition and precipitation kinetics, and membrane morphology.

in the literature, especially regarding whether the selective skin layer results from: (1) nucleation and growth of a small polymer-rich phase followed by coarsening of the nuclei [40]; (2) spinodal decomposition to form nodules at the interface [8]; (3) spinodal decomposition followed by capillary force drive densification in the air-gap region of the dry-wet process [41]; (4) gelation induced via vitrification (glass transition) [42,43]; or (5) crystallization (for crystallizable polymers) interrupted liquid–liquid demixing [10,44]. Despite the controversy on the exact mechanism that controls skin layer formation in hollow fiber membranes, the polymer concentration at the interface with a strong non-solvent will increase rapidly upon contact resulting in a sufficiently high viscosity that a selective skin layer develops. Since the selective skin possesses different properties as measured by *d*-spacing, pore size, or porosity for different separation systems, one may hypothesize that the phase inversion mechanisms to form the selective or functional separation skin are quite different for pore-flow-based membranes (i.e., MF, UF, NF) than for solution–diffusion-based membranes (i.e., RO, gas separation and most pervaporation). The formation mechanisms of loose RO as well as some NF and FO membranes may be a combination of these two mechanisms.

2.2.2. *Phase inversion of semi-crystalline polymers*

The phase separation of a semi-crystalline polymer is more complex because solid-liquid demixing occurs simultaneously with liquid–liquid demixing. There is a clear difference in membrane morphology resulting from liquid–liquid demixing and solid-liquid demixing. Typically, liquid–liquid demixing results in a cellular morphology with pores created from the polymer-lean phase (Fig. 7(a)) that are surrounded by the polymeric matrix created by the polymer-rich phase. In contrast, solid–liquid demixing results in interlinked semi-crystalline particle or globular structures (Fig. 7(d)) [45–47].

The rate of polymer crystallization has to be considered as well. Although the solid-liquid demixing is thermodynamically favorable over liquid–liquid demixing, this does not imply that solid-liquid demixing is preferred kinetically over liquid–liquid demixing. Many previous and recent studies on various semi-crystalline polymers i.e., polylactide [47], nylon [48,49], poly(ethylene-co-vinyl alcohol) [50], polyvinylidene fluoride (PVDF) [51–55] demonstrate that the influence of crystallization on membrane structure is critical when the demixing process is delayed. For example, Sukitpaneenit and Chung [55] found that the coagulant chemistry plays a significant role in determining the final morphology of PVDF hollow fiber membranes. When a strong non-solvent such as water is used as the coagulant, demixing occurs instantaneously and there is insufficient time to induce crystallization. Hence, the liquid–liquid demixing controls the phase separation. However, by introducing weak non-solvents (i.e. alcohols) into the coagulant, the liquid–liquid demixing process is delayed, and the accompanying crystallization process occurs. With increasing alcohol content in the coagulant, the phase separation process is eventually dominated by solid–liquid demixing with a transition from cellular morphology to globular structure as illustrated in Fig 7.

2.2.3. *Limitations of the Flory–Huggins theory for hollow fiber membrane formation*

Although the Flory–Huggins theory for polymer solutions derived in 1942 has been widely adopted for the study of phase inversion during the formation of asymmetric flat membranes. Chung [15] pointed out that the original Flory–Huggins thermodynamics may not be fully capable of describing the appropriate Gibbs free energy for the state of as-spun fibers. It is well known that the major difference

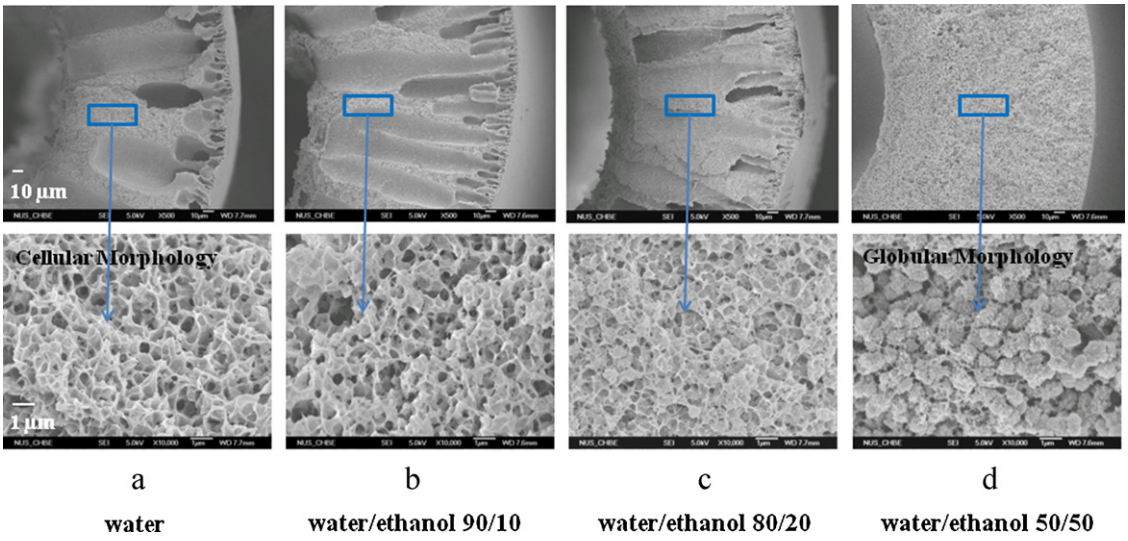

Fig. 7. Cross-sectional morphology of hollow fiber membranes spun from 15 wt% PVDF/NMP with various compositions of water/ethanol external coagulant [55] (Copyright 2009, Elsevier B.V.).

between hollow fiber and flat membrane fabrications is that the phase inversion process for hollow fiber formation usually occurs non-isothermally under tension or elongational stress; the limitations of the Flory–Huggins arise from (1) non-isothermal conditions in the air gap, (2) the additional forces acting on the as-spun hollow fiber solutions (nascent fibers); namely, the gravity-induced force arising from the fiber's mass and the stress applied by the take-up unit, and (3) non-Newtonian viscoelastic fluid behavior along the spinline. Consequently, at least two additional terms have to be included in the equation if the fiber is spun isothermally; one to account for the work done by the external stresses on the nascent fiber and the other an extra entropy change induced by these stresses. The external stresses and viscoelastic behavior may counterbalance their effects on (1) phase instability and separation and (2) molecular orientation. Therefore, future work on mathematical modeling of phase separation should include external stresses and viscoelastic behavior. Otherwise, the models would have very limited applicability.

3. Recent advances in science for the fabrication of hollow fibers

3.1. Macrovoids and state-of-the-art technologies to design macrovoid-free hollow fiber membranes

Macrovoids in textile fibers and membranes fabricated by means of phase inversion are considered to be structural defects. Macrovoids commonly appear as large elongated pores which can grow across the membrane thickness. The presence of macrovoids in membranes provides weak mechanical points which may lead to membrane failure in high pressure or vibrational operation. As a result, compared to commercially available UF and MF membranes full of finger-like macrovoids 20 years ago, most modern UF and MF membranes on the market have a sponge-like structure. However, some researchers still claim that membranes with macrovoid structure can be beneficial in osmotic drug delivery and transdermal delivery systems in terms of transport efficiency [56,57].

The origin of macrovoids is one of the most controversial issues in the study of membrane formation and has been heavily debated in the last four decades among membrane scientists. Some early researchers believed macrovoids originated from instantaneous liquid–liquid demixing and the nucleation of droplets in the polymer-lean phase based on a diffusion-driven mechanism [24,25,35,58–60], while others hypothesized macrovoids arose from a local surface instability, skin rupture and solvent intrusion, followed by the nucleation of droplets in the polymer-lean phase [19,28,61,62]. Other mechanisms such as Marangoni effects [63] and osmotic pressure [64] have been proposed. Krantz and co-workers believe neither diffusion nor Marangoni effects alone can account for the explosive growth of macrovoids [65]. They proposed the solutocapillary convection mechanism which consists of diffusion and Marangoni forces generated by surface tension gradients [66]. The two mechanisms with the greatest acceptance by researchers are: (1) diffusion mechanism with the aid of solutocapillary convection, and (2) local surface instability, skin rupture and solvent intrusion. Both hypotheses have received significant support in the literature [67–71].

Widjojo et al. classified macrovoids in hollow fiber membranes into four types as shown in Fig. 8(a)–(d) [72]; namely, inward-pointed, outward-pointed, elliptical and tear-drop shapes. With enlarged pictures, one can clearly observe the residual traces of non-solvent intrusion for some of the inward- and outward-pointed macrovoids. It is hypothesized that solutocapillary convection and/or osmotic pressure are possible driving forces for the initiation of teardrop and elliptical macrovoids. In contrast, the inward-pointed and outward-pointed finger-like macrovoids most likely arise from non-solvent intrusion, local surface instability, skin rupture or convective flow during rapid precipitation. Recently, a fifth type of

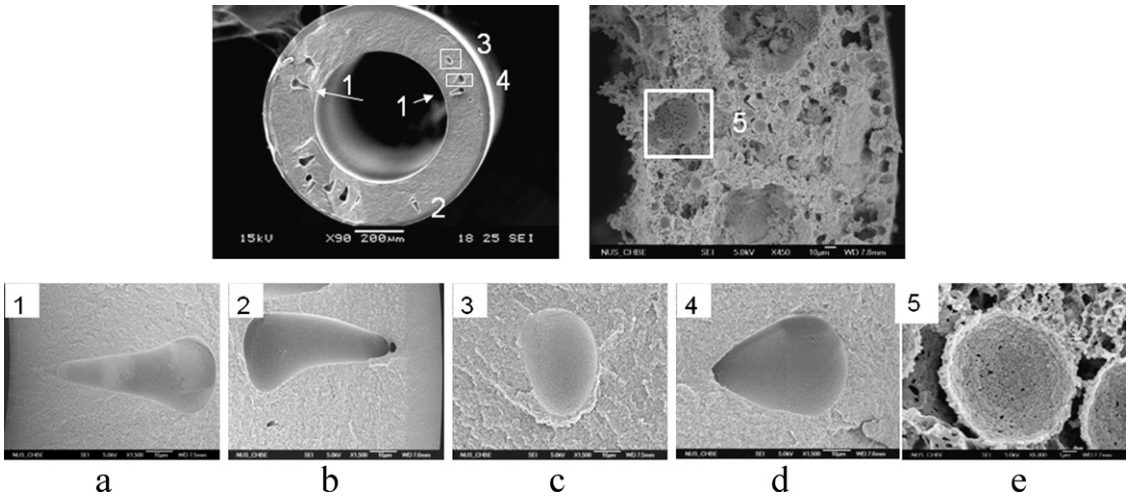

Fig. 8. Five types of macrovoids and trace of intrusion. 1: Inward-pointed [72] (Copyright 2006, American Chemical Society), 2: outward-pointed [72], 3: elliptical [72], 4: tear drop [72], and 5: micelle-like macrovoid [73] (Copyright 2009, Elsevier B.V.).

macrovoid was discovered by Teoh and Chung [73] as illustrated in Fig. 8(e): namely "micelle-like" macrovoids in polyvinylidene fluoride (PVDF) fibers spun from a dope containing 50 wt% polytetrafluoroethylene (PTFE) fine particles of about 1 μm. Two plausible mechanisms for micelle formation are: (1) residual surfactant on the PTFE surface which aids micelle formation and (2) aggregation of air bubbles adsorbed upon the hydrophobic PTFE particles with the aid of non-solvent diffusion and convection [73].

Several approaches have been demonstrated to suppress macrovoid formation, such as: (1) using solutions with high polymer concentrations [3,16] or high viscosity [74] or the addition of high viscosity components [75–77], (2) inducing delayed demixing or gelation [42,64], (3) the addition of surfactants [78], (4) increasing the coagulation bath temperature [14], (5) spinning at high shear rates or high elongational rates [16,79–81], and (6) reducing membrane thickness or annulus flow channel gap of a spinneret [72,82,83]. Examples will be discussed in the following sections.

Cabasso et al. [62] reported that macrovoid formation in polysulfone hollow fibers is strongly dependent on the dope viscosity. They were able to completely eliminate macrovoids when the dope viscosity was increased to 180,000 cP due to the lower tendency for non-solvent intrusion at higher dope viscosity. Kesting et al. [74] claimed that a dope comprising greater than ~30 wt% polymer and a viscosity of greater than about 5×10^4 cP (50 Pa s) at membrane forming temperatures would produce macrovoid-free membranes. However, deviations from their claims were reported. Since the rheological response of a polymer solution depends strongly on spinning conditions, it is difficult to quantify an absolute value of viscosity to produce hollow fiber membranes without macrovoids. With the aid of high take-up speeds, Peng et al. [16] discovered that a dope solution comprising a polymer composition above its critical concentration can suppress macrovoids in hollow fiber membranes. The critical concentration can be obtained by extrapolation from the correlation between viscosity and polymer concentration for different polymers [28]. When the polymer concentration exceeds its critical value, polymer chains tend to form entanglements, which may shift polymer behavior from more fluid-like to more solid-like. Such an entangled network structure may make fibers stronger and hinder non-solvent intrusion if the take-up speed is high and thereby suppress macrovoid formation. In other words, a combination of high viscosity and high take-up speed may create strong negative normal stresses in the radial direction that shrink the hollow fiber thickness and outer circumference. As a result, solvents within the elongated hollow fiber tend to move outward and prevent non-solvent intrusion [16,79–81].

In addition to the effects of viscosity and take-up speed, Husain and Koros [84] found a correlation between macrovoid formation in Ultem/zeolite mixed matrix hollow fiber membranes and the particle size used in dope solutions. They discovered that large particles possibly promote non-uniform phase separation within the mixed-matrix membrane and lead to the formation of macrovoids, while smaller zeolite particles, i.e. 200 nm, can effectively suppress macrovoids which may imply that there is a critical particle size to eliminate particle-initiated macrovoids. Teoh and Chung [73] also reported that particle loading in the dope solution plays an important role in macrovoid formation in PVDF hollow fibers. They found the incorporation of 30 and 40 wt% PTFE particles into the PVDF polymeric matrix reduces finger-like macrovoid formation, but increasing particle loading further to 50 or 60 wt% leads to formation of micelle-like macrovoids.

As discussed previously, air-gap distance and take-up rate could change the thermodynamic state of the polymer solution, create extra phase instability, and facilitate phase separation [15,29]. Thus both factors play important roles in macrovoid formation in hollow fiber membranes. Tsai et al. reported that macrovoids disappeared, reappeared, and disappeared again as the air-gap length increased. They attributed macrovoid reappearance to the effect of

ambient humidity [85]. In free-fall spinning (i.e., drawing occurs solely by the influence of gravity on the mass of the filament), Widjojo et al. observed that increasing air-gap distance exhibits different effects on inward-pointed (shown in Fig. 8(a)) and outward-pointed macrovoids (shown in Fig. 8(b)) [72]. The number and size of the former increase with an increase in air-gap distance because of the time required to develop macrovoids, while those of the latter decrease because of additional moisture adsorption on the outer surface of the nascent fiber in a longer air-gap distance. The adsorbed moisture induces partial precipitation and retards non-solvent intrusion. Peng et al. observed a critical air-gap distance to eliminate macrovoids in high-speed spinning [16]. Above the critical air-gap distance, the effects of die swell and chain relaxation on macrovoid formation can be removed, thus the effects of elongational stretch on chain orientation and negative normal stresses can be established fully along the nascent fiber and eliminate non-solvent (coagulant) intrusion. They found the critical air-gap distances are 5 cm for the PSf/NMP solution (made of 29 wt% PSf in NMP), 5 cm for P84 (28 wt%) and 2.5 cm for CA/NMP (18 wt%) solutions [16].

A thickness dependence of macrovoid formation in flat asymmetric membranes during phase inversion was discovered by Vogrin et al. [82] and Li et al. [83]. Li et al. observed that there is a critical structure-transition thickness, L_c, for macrovoid formation: P84 membranes with a thickness below L_c have fully sponge-like structure, while above L_c have a finger-like structure. Widjojo et al. [72] also observed that macrovoid formation in P84 copolyimide hollow fiber membranes is dependent on the thickness of the spinneret annulus gap. Macrovoids in P84 hollow fiber membranes can be eliminated fully by using a spinneret with an annular gap of 0.1 mm—the critical thickness was found to be ~105 μm (Fig. 9(a1)). Interestingly, the critical wall thickness to produce macrovoid-free P84 hollow fibers is much higher than that to produce macrovoid-free P84 asymmetric flat membranes (i.e., 105 μm vs. 11 ± 2 μm) [72,83]. This is due to the difference in phase inversion processes between hollow fibers and flat-sheet membranes. The inner and outer skins of the wet-spun hollow fiber coagulate almost immediately upon exiting the spinneret and precipitate in the water filled coagulation bath, while the asymmetric flat membrane is cast on a glass plate and the top free surface is exposed to air for a short period of time. As a result, the outer surface of the nascent flat membrane can move slightly up or down during coagulation and accommodate macrovoid formation via various mechanisms underneath the skin surface. The free surface and associated ability to accommodate different macrovoid formation mechanisms in the asymmetric flat membrane lead to a smaller critical structure-transition thickness to eliminate macrovoids because of the lack of super saturation [66]. Furthermore, compared with hollow fiber spinning, the asymmetric flat membrane experiences much lower shear stresses and shorter exposure time to shear stresses during membrane casting. Past literature has demonstrated that shear stresses within the spinneret can change the state of the fluid and suppress macrovoid formation [72]. Therefore, hollow fibers extruded from a small annular gap would experience higher shear rates and stresses that would result in higher molecular orientation and chain packing, both factors confound macrovoid formation.

3.2. Origins of irregular contours of hollow fibers and technologies to remove the irregularities

Irregular shapes formed in hollow fiber membranes from conventional spinnerets are undesirable and generally affect the performance and mechanical strength of the fiber. Fig. 9(c) and (d) and Fig. 10 display some images of hollow fibers with irregular shapes. The irregularities in the fiber's shape may be classified into: (1) ovality, (2) poor concentricity, and (3) wavy or deformed membrane cross-section. Ovality may be overcome by increasing the phase inversion duration so that the nascent fiber precipitates completely and is able to withstand the stress along the guide rolls of the spinline. Poor concentricity may be resolved by properly cleaning the spinneret and aligning the central bore fluid needle. However, the formation mechanism of an irregular internal contour is complicated and challenging.

Irregularity of the hollow fiber lumen has been reported in the literature and attributed to die swell and its correlation with spinning conditions [34,86–92]. Van't Hoff [34] reported that the irregular inner shape was strongly affected by bore fluid volume and composition. In the spinning of PES/NMP/glycerol (30/65/5 wt%) dope solutions, they found that an increase in glycerol concentration in the bore fluid induces lumen irregularity because the increase in bore fluid viscosity leads to insufficient liquid supply to the fiber lumen. Similar phenomenon was observed by Roesink [87] in the PEI/polyvinylprrolidone (PVP) hollow fiber. Van't Hoff also revealed that the irregular inner shape can be found when pure water was used as the bore fluid [34], and the irregularity can be reduced by increasing NMP content in the bore fluid to 50 wt%. In high speed spinning of polysulfone (PSf) hollow fiber, Santoso et al. [92] confirmed the above phenomena and attributed the deformed lumen contour to either bore fluid deficiency or rapid formation of a dense inner skin caused by the use of a strong non-solvent (i.e. water) as the bore fluid. The former results in lumen vacuum and creates wavy inner contours but can be addressed easily by increasing the bore fluid flow rate, while the latter can be resolved by increasing solvent content so that the nascent lumen undergoes delayed demixing and is able to accommodate the stresses and strains that occur during phase inversion. In addition to using the delayed demixing approach, increasing polymer concentration in the spinning dope is another approach to minimize the lumen irregularity as demonstrated by Yan [88], McKelvey et al. [89] and Pereira et al. [90]. However, this approach may also increase the substructure resistance and reduce membrane separation performance efficiency.

Bonyadi et al. [93] were the first to analyze possible mechanisms for the formation of an irregular lumen contour and offered two hypotheses: (1) mass transfer and hydrodynamic instability and (2) elastic and buckling instability. The first may occur in the air-gap region where the bore fluid comes into contact with the polymer solution and creates an inward motion of a perturbed interface,

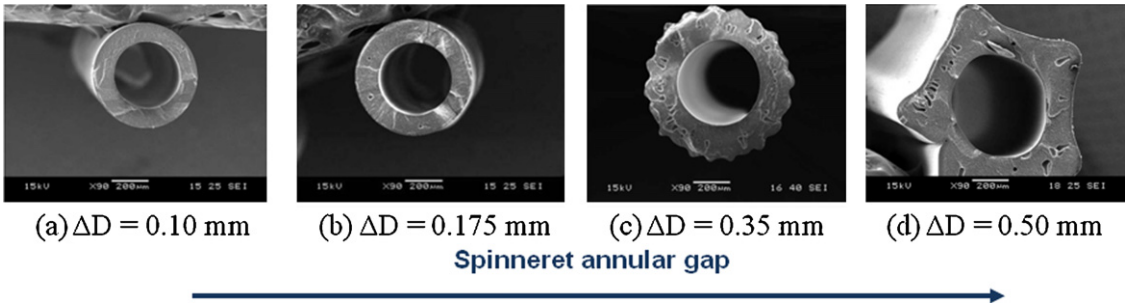

Fig. 9. Effect of spinneret design on macrovoid formation [72] (Copyright 2006, American Chemical Society).

while the latter occurs immediately when fiber enters the coagulation bath. They concluded that the elastic and buckling instability is the primary mechanism for formation of an irregular inner surface. As illustrated in Fig. 10, the observation of a non-uniform cross-sectional geometry is in good agreement with the predicted post-buckling shapes of a long elastic shell predicted by Greenhill using elastic theory [94]. Other models also have been proposed recently. Shi et al. correlated a viscoelastic Mach number with the deformation of irregular inner contour [95,96], while Yin et al. modeled the formation of a grooved shape in the lumen side of hollow fiber membranes and attributed the mechanism to a Marangoni instability [86].

In addition to the irregular inner-layer contour, hollow fibers with outer surface irregularity spun from conventional spinnerets also have been reported [72,97]. Widjojo and Chung [72] observed fascinating star and gear profiles of P84 during wet-spinning. These deformations were eliminated by decreasing spinneret annular gap thickness, increasing air-gap distance or elongational stress. Zhang et al. [97] found that the inner contour of polyacrylonitrile (PAN) hollow fibers is more likely to be circular than the outer with varying air-gap distances due to the partially induced phase separation and uneven surface tension in the air-gap region.

Though the formation of irregular shapes in hollow fibers is complicated and generally undesirable, the beauty of R&D in hollow fiber formation is that most irregularities can be removed by investigating their origins, understanding the science, and then revising spinning conditions. An increase in dope viscosity (by increasing polymer concentration or using additives), solvent concentration in bore fluid, and air-gap distance are easily implemented solutions that offer great potential for eliminating the irregularity.

4. Evolution of hollow fiber fabrication technologies for sustainability applications

4.1. Hollow fiber membranes with an ultrathin selective or separation layer

In addition to having a fully porous substructure and decent configurations without irregular shapes, high permeation flux and separation factor are critical for hollow fiber membranes used for sustainability applications such as energy development and gas separation, biofuel production and pervaporation, water reuse and wastewater recycle, and CO_2 capture. Therefore, fabrication of hollow fibers with an ultrathin selective or separation layer is essential because an ultrathin selective layer reduces mass transfer resistance (i.e., increases permeation flux) which reduces energy consumption and the overall footprint of the process.

Because of the complexity of the phase inversion process and the trade-off between the formation of an ultrathin selective layer and the generation of defects [3–8,13,32,98–101], the production of hollow fibers with an ultrathin selective layer is challenging. This is especially

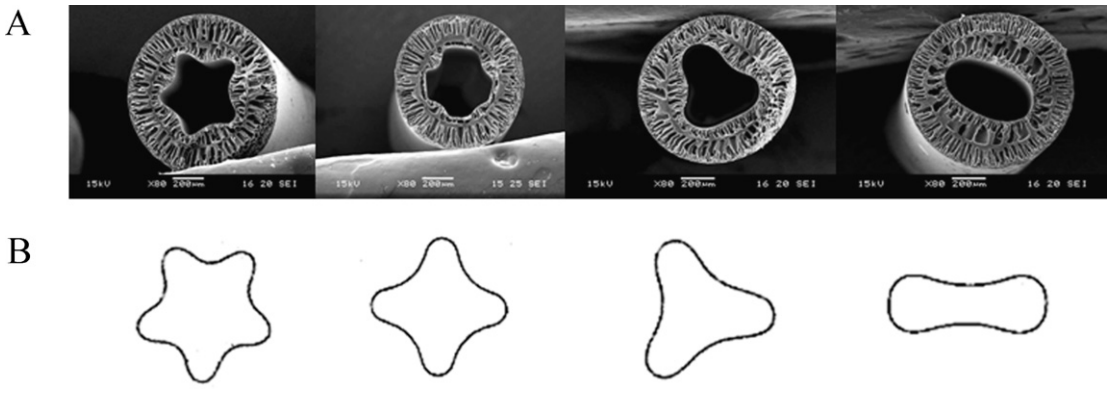

Fig. 10. Close agreement between the spun fibers cross sectional geometry (a) and the predicted postbuckling shapes of a long elastic cylindrical shell (b) [93] (Copyright 2007, Elsevier B.V.).

true for energy development, gas separation and CO_2 capture membranes due to the fact that gas molecules are small (Angstroms in size) and very sensitive to defects in the functional layer. However, significant advancements in fabricating membranes with distinguished gas separation performance have been made during the past three decades. In the late 1980s, Kesting et al. [74] invented the Lewis acid:base complex spinning solutions and developed a new generation of asymmetric hollow fibers with an ultra-thin and graded dense skin. The Lewis acid:base dope formulation is a unique solvent that has a large combined molar volume but is very unstable in water. The large molar volume may create a large residual free volume after these solvents leach out from the nascent membrane, while the instability in water facilitates phase separation and minimizes the presence of residual solvents in the membrane. These characteristics are essential to produce membranes with a high free volume, ultra-thin dense layer. Kesting and co-workers reported that the oxygen permeability of polysulfone membranes using propionic acid as the Lewis acid increased by a factor of 2–4 without sacrificing O_2/N_2 selectivity. In 1990s, Chung et al. [28] also fabricated polyethersulfone hollow fibers with an ultrathin dense layer of 474 Å. They proposed the key process variables were the chemistry and flow rate of the bore fluid, and the use a dope exhibiting significant polymer chain entanglement. The chain entanglement helped the formation of a less defective selective skin, while the solvent rich bore fluid led to delayed demixing and a fully porous substructure. For the hollow fibers fabricated by Kesting et al. [74] and Chung et al. [28], a silicon rubber coating has to be employed to seal the defects on the dense-selective layer and regenerate the selectivity. Clausi and Koros [100] produced defect-free Matrimid gas separation hollow fibers with an ultra-thin selective layer of around 1000 Å using a Matrimid solution comprising volatile and non-volatile solvents and a non-solvent. They hypothesized that the fast removal of the volatile solvent at elevated temperatures (50 °C) from the polymer matrix helped reduce the formation of defects. The same practice with the addition of a non-solvent (either water, tetrahydrofuran (THF) or ethanol) was adopted to fabricate defect-free asymmetric hollow fiber membranes from other polymers e.g. polyamide-imide polymer at 50 °C, as reported by Kosuri and Koros [101]. Most recently, Peng and Chung [102] took another approach without using a non-solvent and high temperatures but by designing spinnerets with different dimensions and fabricated defect-free Torlon® 4000TF gas separation membranes with a dense layer thickness of 540 Å. Their approach was based on appropriate control of shear-induced and elongation-induced polymer chain orientation during spinning by varying the spinneret dimension and adjusting the take-up rate.

Since Henis and Tripodi invented the silicone rubber coating technique to restore the selectivity of a defective ultrathin dense-selective layer, other coating techniques for asymmetric hollow fibers have been developed for various sustainability applications [103–110]. Instead of using silicone rubber, one can employ a similar coating technique but deposit an ultrathin selective layer upon an asymmetric membrane to enhance its separation performance [8,11,12,103–109]. The keys to deposit a defect-free ultrathin layer on top of a hollow fiber substrate for gas separation and pervaporation are to (1) employ a strong substrate which has a smooth surface and a fully porous substructure, (2) choose a substrate that has a very small surface pore size, and (3) prevent intrusion during coating using a pre-wetting agent or other means.

Co-extrusion technology for dual-layer hollow fiber spinning offers a new manufacturing paradigm to exploit expensive, high-performance materials as the selective layer and/or reduce substructure resistance through use of another material or less concentrated polymer solution as the inner layer. In the late 1980s, Kuzumoto and Nitta invented the co-extrusion method and extruded inner and outer dope solutions containing the same polymer for water reuse [111]. Ekiner et al. extended this work to the production of gas separation membranes [112]. The mechanism and control parameters for dual-layer hollow fiber formation are complex because phase inversion of polymer solutions with different chemistry and rheological properties occurs simultaneously. In addition to the guidelines for spinning single-layer hollow fibers, i.e., varying the dope composition, air-gap distance and take-up speed, extensive experimental results show that the outer-layer flow rate plays an important role in determining the overall gas permeation flux and selectivity of dual-layer hollow fibers [113–117]. Generally, a decrease in outer-layer flow rate can enhance permeance by reducing the dense-selective thickness in the outer layer but also can lead to a more defective selective layer. Ekiner et al.'s early work at DuPont is informative because the membranes developed are delamination-free at the interface and have good gas separation performance [112]. Suzuki et al. [114] also fabricated dual-layer hollow fiber membranes composed of a dense polyimide outer layer and a sponge-like inner layer made of another polyimide for CO_2/N_2 separation. Recently, Li et al. [118] and Peng et al. [119] used the strategy of replacing the inner layer with the same polymer but at a lower concentration, and successfully produced dual-layer PES and Extem® (polyetherimide) hollow fiber membranes with an ultrathin selective layer of less than 1000 Å. The advantages of using the same material and a lower inner polymer concentration are to develop a seamless interface and to significantly reduce the substructure resistance, respectively. The seamless interface can enhance the fiber's long-term integrity, while the reduced substructure resistance increases membrane permeance.

Through proper control of processing conditions, the ultrathin selective layer may be formed at the interface between the two layers. The mass transfer and phase separation in such a process are significantly more complicated than that resulting in an outer selective layer. For example, Jiang et al. discovered that the interfacial layer between PSf and Matrimid® was the separation layer for biofuel (tert-butanol) separation with pervaporation performance comparable to ceramic membranes [120]. The inter-diffusion of highly miscible PSf and Matrimid® molecules was the driving force to form the ultra-thin interpenetrated functional layer. Therefore, with appropriate choices of miscible or partially miscible blend pairs, one may be able to design on a molecular level

high-performance hollow fiber membranes with an ultrathin internal separation layer by means of dual-layer co-extrusion technology. Recently, Kopec et al. [121] fabricated and cross-linked asymmetric composite hollow fiber membranes simultaneously using the dual-layer spinneret approach.

Hollow fiber membranes with an ultrathin dense-selective layer produced from both single-layer and dual-layer spinning are in principle applicable to the separation of natural gas as long as the membranes are stable at high temperatures and have resistance to CO_2-induced plasticization. Hollow fibers made from some special polyimides have shown good performance and reliability in the separation of natural gas [102,122–127]. Cross-linking and heat treatment are the common methods to enhance CO_2 gas selectivity and improve anti-plasticization properties but with some sacrifice in gas permeance [122–127].

In addition to polyimides, new membrane materials such as thermally rearranged polymers (TR polymers) [128,129], polymers with intrinsic microporosity (PIM) [130,131], room temperature ionic liquids (RTILs) [132–134], mixed matrix membranes containing metal-organic frameworks (MOFs) [135,136], and PEO materials [137–140] have been invented for natural gas and flue gas separation with superior separation performance. However, there are challenges to process these high-performance materials into commercially viable hollow fiber membranes. Similar to the processing of conventional polymer materials, the fundamental guidelines to produce single-layer hollow fibers from these materials are to: (1) synthesize these materials with reasonably high molecular weights, (2) prepare spinning solutions with a high viscosity, (3) investigate phase diagrams and optimize dope compositions, and (4) use a moderately high air-gap distance and take-up speed to increase polymer chain orientation and assure good productivity. However, fabrication of composite hollow fiber membranes using these materials is another option. Composite hollow fiber membranes can be produced by dual-layer spinning using high-performance materials as the thin outer layer following the general protocols to produce dual-layer hollow fiber membranes. Coating the high-performance materials onto a single-layer hollow fiber support is another approach, where pore size and porosity of the substrate have to be carefully controlled to prevent intrusion of the coating material as well as to minimize the substructure resistance [106,141].

The selective layer thickness for water-based separations such as membrane distillation (MD), UF, and NF, which do not rely on a solution–diffusion separation mechanism, is not as well defined as for gas separation membranes. A direct measurement approach such as scanning electron microscopy (SEM) or transmission electron microscopy (TEM) may be used to measure the thickness of the functional layer for these membranes. As discussed in Section 2.2, the control parameters to form a truly dense layer or loose dense layer with a desired pore-size distribution could be very different. However, properly tuning the dope composition by adding pore-forming agents or non-solvent components and use of the co-extrusion approach can facilitate the formation of a thin functional layer and enhance membrane permeance.

4.2. Mixed matrix hollow fiber membranes for energy development and gas separation

Since the intrinsic properties of membrane materials govern the spinnability and separation performance of hollow fiber membranes, proper design and choice of membrane materials are critical to produce hollow fibers with superior separation performance. Mixed matrix membranes (MMMs) consisting of (1) different polymers or (2) polymers embedded with inorganic or organic materials are a promising approach to develop new materials for a wide range of applications [142–146]. It is believed that MMMs can surpass the Robeson trade-off line [147] if the nano-size fillers are incorporated intelligently within a continuous polymeric matrix.

Successful development of MMM hollow fiber membranes will require homogenous distribution of the molecular sieves or nano-particles within the dense-selective layer to utilize fully the unique characteristics of the filler. Jiang et al. [148] have demonstrated that a majority of molecular sieves tend to locate in the middle of the porous supporting layer in single-layer MMM hollow fibers where the molecular sieves cannot improve gas separation performance. Therefore, the dual-layer spinning technology may offer significant advantages. In addition to lowering the material cost, dual-layer spinning offers the potential to place the nano-particles only in the thin outer layer. The desirable structure of a hollow fiber with a mixed matrix skin is shown in Fig. 11, where the highly selective particles are fully dispersed in the outer skin region of the membranes.

The development of MMM dual-layer hollow fiber membranes was initially carried out by Miller et al. [149], Ekiner and Kulkarni [150], and Koros et al. [151]. Miller et al. [149] spun blend materials comprising polyaramide, polyimide or cellulose with silicalite or ZSM-5 for the separation of p-xylene and m-xylene mixtures. Ekiner and Kulkarni [150] produced hollow fibers made of Ultem/chabazite type (CHA) molecular sieves (pore size 3.8 Å) with an O_2 permeance of 7.4–9.5 GPU and an O_2/N_2 selectivity ranging from 8.1 to 8.5. Koros et al. [151] modified the zeolite surface with silane to improve compatibility between the particle and the polymer. These pioneering studies were reported in patents without the scientific and engineering detail typically found in refereed journal publications.

Strategies for fabricating dual-layer hollow fibers with a thin outer layer of mixed matrix materials and enhanced gas separation performance were developed by Jiang et al. [137], Li et al. [152], Husain and Koros [153], Shu et al. [154,155], and Widjojo et al. [156]. Jiang et al. [148] adopted heat-treatment and a two-step coating process to densify the outer mixed matrix layer. The resultant hollow fibers showed significantly enhanced He/N_2 and O_2/N_2 selectivity compared to neat polymer membranes. However, the calculated mixed matrix dense-selective layer thickness was around 2.5 μm based on the intrinsic O_2 permeability of corresponding flat, dense polysulfone–zeolite beta MMMs. Li et al. [152] fabricated dual-layer PES/P84

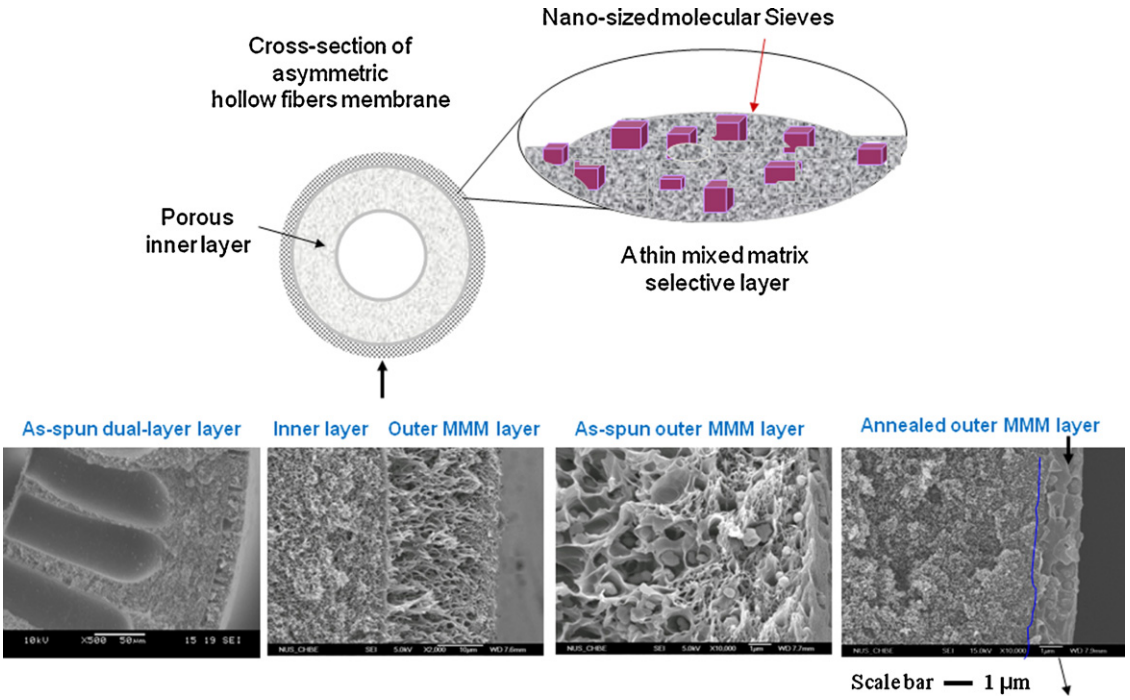

Fig. 11. Schematic cross-section morphology of the dual-layer hollow fiber with a polymer/particle mixed matrix skin.

hollow fiber membranes with a PES–zeolite beta mixed matrix dense-selective layer of 0.55 μm by adjusting the ratio of outer layer flow rate to inner layer flow rate followed by heat-treatment at 235 °C using a two-step coating. The dual-layer hollow fibers possessed O_2/N_2 and CO_2/CH_4 selectivities ~10–20% greater than that of neat PES dense films.

By increasing the hydrophobicity of the zeolite via capping surface hydroxyls with hydrophobic organic molecules, Husain and Koros [153] showed significant selectivity enhancement of 10% for O_2/N_2, 29% for He/N_2, 17% for CO_2/CH_4 based on pure gas measurements and 25% for mixed gas measurements with CO_2/CH_4 mixtures for polyetherimide MMM hollow fibers relative to the neat polymer. Shu et al. [154,155] synthesized nanostructured zeolite particle surfaces by a halide/grignard route. They improved the interfacial interaction between the zeolite nanoparticles and the polymer matrix as well as reduced chain rigidity and enhanced overall separation performance of the MMMs.

Jiang et al. [148] and Li et al. [152] proposed using glassy polymers with relatively low T_g (e.g. PSf and PES) for the mixed-matrix layer and glassy polyimides with high T_g (e.g. Matrimid and P84) for the support layer. Such a combination permits annealing of the mixed matrix outer layer without significant compaction of the porous support and associated reduction in permeance. Such an approach eliminates interfacial voids but is not economically viable because high cost polyimides are required for the support layer. Widjojo et al. [156] introduced a novel method to rectify this problem by utilizing a blend of polyethersulfone (PES) and low cost Al_2O_3 nano-particles to replace the expensive polyimides as the supporting layer. The incorporation of 20 wt% zeolite beta in the outer selective layer and 60 wt% Al_2O_3 in the inner layer under appropriate spinning conditions enables the fiber to retain its porous substructure even after annealing above the neat polymer glass transition temperature.

In addition to dual-layer co-extrusion technologies, pre-coating nano-particles with a charged polymer can prevent nanoparticle agglomeration during the spinning of mixed matrix hollow fibers [157]. Moreover, doping the zeolite with Ag^+ can enhance the membrane CO_2/CH_4 selectivity [158]. However, extensive experiments indicate the improvement in productivity (permeance and selectivity) is significantly smaller than expected based on predictions of the Maxwell equation. To produce high-performance mixed matrix hollow fiber membranes, the dense-selective layer thickness must be reduced further and an agglomeration-resistant filler smaller than 20–30 nm used [145,157]. Mixed matrix hollow fibers made from materials blending on the molecular level are preferred [135,136,139,140].

4.3. Less-swelling membranes for biofuel and other aqueous solvent separations

The basic knowledge and fabrication technology for hollow fiber gas separation membranes discussed in Section 4.1 can be adopted to produce hollow fibers for the pervaporation of biofuels (mainly refers to ethanol and buthanol) from fermentation broths and other aqueous solvent mixtures. Careful tuning of dope and bore fluid compositions, proper control of spinning conditions, and

appropriate post-treatment methods are critical to produce hollow fiber pervaporation membranes with high separation performance. The major difference between gas separation and solvent separation is the high solubility of the solvents that can result in detrimental membrane swelling and damage to the dense-selective layer. Therefore, the challenges of developing membranes for biofuel and other solvent separations are to enhance (1) resistance to feed-induced swelling, (2) chemical and thermal stability, and (3) long-term mechanical integrity. In addition to a desirable morphology produced by optimizing spinning conditions, materials with superior physiochemical properties and chemical resistance are essential to achieve stable separation performance [159–168].

Asymmetric hollow fiber membranes for biofuel dehydration have been made from various hydrophilic polymers such as polyvinyl alcohol [160], polyvinyl alcohol/sodium alginate [161,169], perfluorosulfonic acid/polyvinyl alcohol [170], cellulose acetate (CA) [171], polypropylene grafted with poly (acrylic acid) [161], chitosan/polyacrylonitrile (PAN) [172], cellulose acetate (CA)/chitosan [163], PAN [173], polyimides [164], PBI and its blends [165,166], and polyamide-imides [174,175]. In dehydration, polyimides and PBI have shown great potential. The former possesses a desirable separation factor and anti-swelling properties [174–176], while the latter is a high-temperature material with superior hydrophilic characteristics and good chemical resistance [165,166].

Since single-layer hollow fibers may suffer severe swelling when exposed to the feed solution and lose selectivity, the use of anti-swelling materials as the inner support layer can improve overall separation pervaporation performance and long-term stability. Jiang et al. [120] and Wang et al. [175] describe two most prominent examples of this approach. The former demonstrated PSf/Matrimid® dual-layer hollow fiber membranes with an outstanding separation performance that far surpasses the existing polymeric membranes and approaches ceramic membranes for *t*-butanol dehydration. The latter developed polyamide-imide (Torlon®)/polyetherimide (PEI) hollow fiber membranes for dehydration of C_1–C_4 alcohols. In addition to the unique dehydration properties of the selective layer made of PSf/Matrimid blends or Torlon®, the superior performance of the dual-layer hollow fibers was attributed to (1) the low water uptake and swelling resistance of the support layer and (2) the desirable membrane morphology consisting of a fully porous inner layer and an ultrathin dense-selective skin.

The swelling resistance of dual-layer hollow fiber membranes made of polyimides can be enhanced further by cross-linking. Liu et al. [177] fabricated P84/polyethersulfone (PES) dual-layer hollow fiber membranes for IPA dehydration. They reported that the separation factor can be improved from 50 to 953 after the fibers were cross-linked by a p-xylenediamine solution for 2 h. Shi et al. [178] combined heat treatment and cross-linking to improve the stability and separation performance of dual-layer PBI/P84 hollow fiber membranes for acetone dehydration. Mixed matrix hollow fibers consisting of components with different physicochemical properties mixed on a molecular level have been reported recently for biofuel separation. Two examples of this approach are molecular level MMMs comprising POSS or CD for biofuel dehydration [179,180].

In contrast to biofuel dehydration, little effort has been devoted to the development of asymmetric hollow fiber membranes for biofuel recovery using hydrophobic membranes. Most hollow fiber membranes reported in the literature are composite membranes comprising a thin layer of PDMS coated on a porous support made of a stronger material [181]. Recently, an asymmetric PVDF hollow fiber membrane for ethanol recovery was developed by Sukitpaneenit et al. [182,183]. Preliminary results indicated that the membrane possesses impressive performance with an extraordinary total flux and reasonable separation factor for ethanol–water separation. Clearly, significant opportunity exists for future development of asymmetric hollow fiber membranes for biofuel recovery.

4.4. Functional membranes for membrane forward osmosis (FO) and distillation (MD) used for water reuse and desalination

Forward osmosis (FO) and membrane distillation (MD) are emerging membrane technologies for water reuse and desalination. The former is an osmotic pressure driven process, while the latter is a temperature-driven one [184,185]. The molecular design of FO membranes with superior separation performance requires control of pore size or interstitial molecular space to values comparable to water's molecular size (≅0.278 nm) because the solution–diffusion mechanism is dominant in desalination processes [186]. In some cases, FO membranes for water reuse may prefer high fluxes and tolerate pore sizes up to 0.35 nm. Hence, pore-flow mechanisms may influence separation performance [187] and nano-filtration (NF)-based FO membranes may be suitable.

To produce hollow fiber FO membranes, both single- and dual-layer spinning technologies have been employed by using polybenzimidazole (PBI) [188–190] or cellulose acetate [191,192] dopes at or above the critical concentration, followed by thermal annealing or chemical cross-linking in order to minimize defects. For decades, thin film composite (TFC) membranes with high salt rejections have been used in RO processes [193–196]. Commercially available TFC-RO membranes consist of three layers: (1) a thin polyamide layer as a selective layer, (2) a porous polysulfone layer as the intermediate layer to facilitate formation of the selective layer and improve interactions with the underlying non-woven fabric, and (3) a thick layer of a non-woven fabric as the mechanical support layer to withstand the required operating pressures. Apart from the polyamide layer, the other layers are hydrophobic in nature. McCutcheon and Elimelech [197] have explored use of conventional TFC-RO membranes in FO applications. They found that TFC-RO membranes show severe internal concentration polarization. This dramatically reduces the water flux in FO processes as the hydrophobic sub-layers tend to hinder osmotically driven water diffusion cross the

membrane and the thick non-woven fabric creates an additional diffusional resistance.

The preferred support layer for FO membranes would be as thin as possible or non-existent with minimal resistance to osmotically driven water transport [188–192]. By eliminating the non-woven fabric used in traditional TFC-RO membranes, Yip et al. [198] and Wang et al. [199] pioneered the fabrication of TFC-FO flat-sheet and hollow fiber membranes, respectively, using polysulfone and polyethersulfone supports, respectively, for FO applications. They claim that the ideal support substrate for TFC-FO membranes would comprise a thin, sponge-like structure on top of a fully finger-like sub-structure. Recently, Wang et al. [200] and Widjojo et al. [201] studied TFC flat membranes with support layers comprised of blends of hydrophilic sulfonated polysulfones and hydrophobic polysulfones. Both reported water fluxes in the pressure retarded osmosis (PRO) mode using seawater as the feed that exceeded the highest values reported previously in the literature. Additionally, Widjojo et al. found that macrovoids are not essential for high flux. However, the hydrophilic sublayer is critical because it minimizes internal concentration polarization. The aforementioned findings should be investigated in the hollow fiber configuration.

In contrast to FO, MD membranes require a non-wetting, microporous, hydrophobic membrane to serve as the barrier between the feed and permeate solutions [184,202–213]. Porous membranes produced from such materials can permit water vapor transport across them and condensation into the cold permeate stream while suppressing pressure-driven liquid flow. The preferred MD membrane would possess (1) high surface and bulk porosity with surface pores in the range between ultrafiltration and Knudsen diffusion, (2) high hydrophobicity but a thin wall to enhance flux as well as low thermal conductivity to minimize temperature polarization and heat loss, and (3) long-term mechanical and performance stability with low fouling. Melt spun and stretched polypropylene Celgard membranes have been used in first generation MD systems. However, hydrophobic polymers, especially polyvinylidene fluoride (PVDF), and copolymer poly(vinylidene fluoride-co-hexafluoropropylene) (PVDF-HFP), have great potential and dominate recent MD studies. The single-layer and dual-layer spinning guidelines described previously have been used to develop MD hollow fiber membranes with high fluxes and tailored morphology from neat polymers and mixed matrix materials containing PVDF and various kinds of nanoparticles [205,209–216]. For example, adding hydrophobic particles into the dope solution can enhance membrane hydrophobicity and simultaneously suppress marcrovoid formation to enhance long-term performance stability. High solvent concentrations in the bore fluid can facilitate formation of the porous substructure and result in high permeation fluxes while changes in air-gap distance and take-up rate can tailor the pore size of the selective layer. Furthermore, carefully optimizing the fiber wall thickness by adjusting the flow rate or other approaches can enhance the mass transfer and thermal efficiency of the MD process.

5. Emerging R & D on hollow fiber formation

5.1. Spinneret design

Spinneret design plays a critical role in determining molecular orientation and membrane morphology of the resultant hollow fiber membranes. A common spinneret design consists of a reservoir and an annular channel which has a high annulus length/flow gap ($L/\Delta D$) ratio to ensure a stable flow of the polymer solution. When a viscous polymer solution is extruded through the spinneret, it is subjected to various stresses which influence the macromolecular chain orientation and packing. Moreover, the rheological properties of the polymeric solution determine molecular relaxation time and die swell. These factors control membrane formation, morphology, and ultimate separation performance.

Membrane researchers have attempted to exploit the influence of spinneret design on membrane formation and performance. This work includes design modifications to (as summarized in Fig. 12) (1) tailor pore-size distribution and control pure water permeability of ultrafiltration hollow fiber membranes by fabricating spinnerets with different flow angles (Fig. 12(b)) [217], (2) nearly double the surface area of hollow fiber membranes for gas separation by designing a spinneret with micro-fabricated inserts to create corrugated patterns in the outer fiber perimeter (Fig. 12(c)) [218], (3) enhance gas separation performance by varying the spinneret dimension [102], and (4) induce interlayer diffusion at the interface of dual-layer hollow fiber membranes by an indented middle tube (Fig. 12(d)) and thereby eliminate delamination [219].

Traditional spinnerets may not be applicable for the spinning of dope solutions made of hyperbranched polymers because of their distinct non-Newtonian fluid behavior and long relaxation times [220]. Widjojo et al. [221] designed spinnerets to address these differences by modifying the exit channel geometry to reduce the shear-induced flow instability and die-swell that occurs during solution spinning of hyperbranched polymers. They demonstrated that short conical spinnerets with a flow angle of 60° (Fig. 13(d)) as well as short, round flow-channel spinnerets with a flow angle of 30° (Fig. 13(e)) can reduce or eliminate extrudate distortions. Çulfaz et al. [222] recently reported the fabrication of PES hollow fiber membranes using a spinneret with a micro-structured needle. Under optimal spinning conditions, the resultant hollow fibers possessed micro-structured inner surfaces with a reasonably narrow pore-size distribution, uniform skin layer, increased membrane area-to-volume ratio, and enhanced flux per module volume.

In addition to conventional single-layer and dual-layer hollow fiber configurations, design of rectangular or tubular membranes with multiple channels may enable new opportunities for membrane technology in water reuse. Toshiji pioneered the use of solution spinning processes for the production of hollow tape-shaped membranes [223]. Hallmark et al. developed a melt spinning process for microcapillary films embedded with a number of hollow capillaries [224]. Peng et al. produced ultrafiltration rectangular membranes with multiple hollow

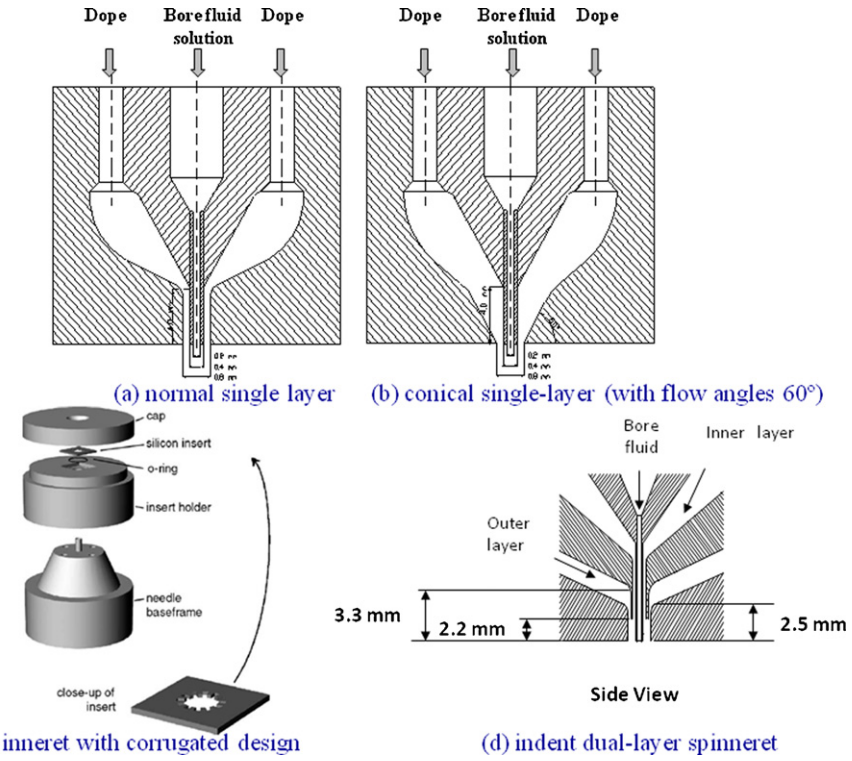

Fig. 12. Schematic diagrams of spinnerets with various designs [217] (Copyright 2004, Elsevier B.V.), [218] (Copyright 2005, Elsevier B.V.), [219] (Copyright 2007, Elsevier B.V.).

holes via a non-solvent-induced phase inversion process [225]. For multi-channel hollow fibers, IMT has developed and commercialized a multi-bore membrane comprising seven channels of 0.9 mm inner diameter in one fiber [226]. This novel membrane structure is much stronger than a single-bore hollow fiber. However, additional fundamental process development is required because formation of these multi-channel membranes involves

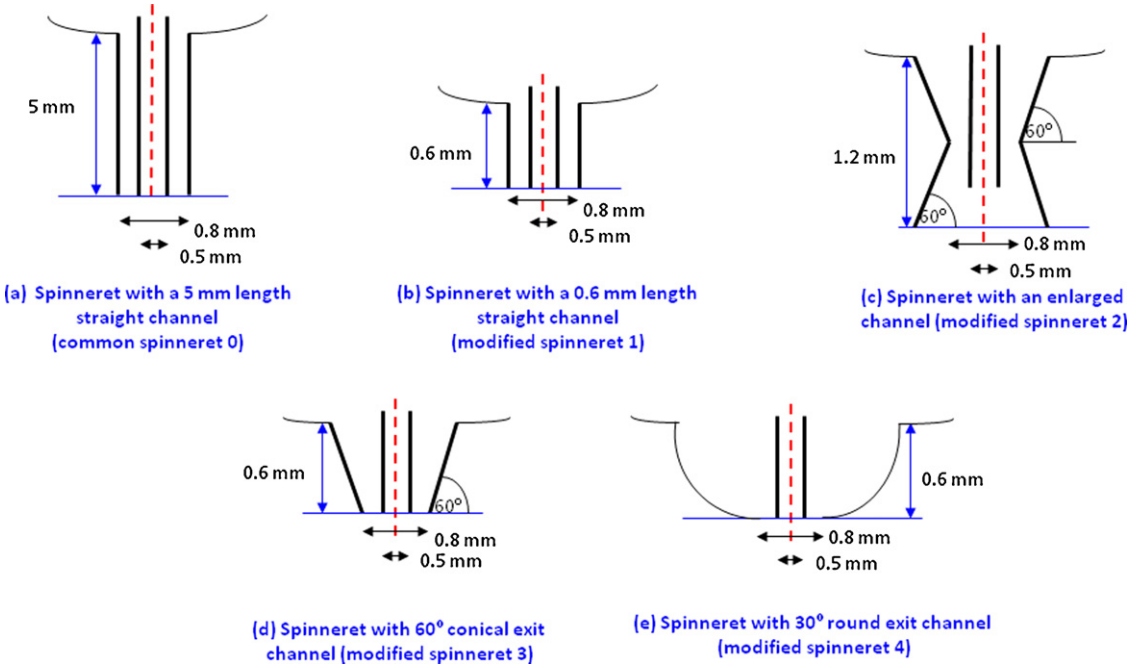

Fig. 13. Schematic diagrams of the exit channel designs of common spinneret and four modified spinnerets [221] (Copyright 2010, Elsevier B.V.).

complex, multi-component mass transfer and is poorly understood.

In addition to spinneret design, optimizing membrane fabrication requires knowledge of the relationships between polymer structure, dope rheology, process conditions, phase inversion, and ultimate hollow fiber performance. Integrating spinneret design with other physicochemical factors is critical to enhancing hollow fiber membrane performance and providing the basis for development of future membranes from newly developed polymeric materials.

5.2. Rheology

Rheology dictates fluid behavior during spinning, stability of the spinning process, and production of hollow fibers with desirable separation properties [227]. Spin dopes experience shear stresses within the spinneret and the extruded nascent fibers experience elongational stresses in the air-gap region that determine chain packing and morphological architecture of the final hollow fiber membrane. However, the importance of rheology largely has been ignored in membrane formation. This likely is due to the complex non-Newtonian behavior of high-molecular-weight polymer solutions.

The effects of shear rates or stresses within the spinneret on membrane morphology and separation performance were studied by Qin et al. for water reuse [228], Chung et al., East et al., and Shilton et al. for gas separation [229–231], Ren et al. for natural gas purification [232], and Liu et al. for isopropanol dehydration [177]. For ultrafiltration membranes, both pore size and surface roughness decrease with an increase in shear rate [228]. As a result, flux decreases but rejection increases with increasing shear rate. Similar relationships were found for pervaporation and gas separation membranes as shear-induced orientation may tighten the pore size and enhance selectivity. However, once a critical shear rate is exceeded, the effect of shear thinning on dope viscosity may induce defects and be detrimental to separation performance.

The relationships between elongational stress, fluid viscoelasticity, hollow fiber formation, and separation performance are complex. Ekiner and Vasilatos were the first to study the effect of elongational viscosity for polysulfone/DMAc and polyaramide/DMAc spin dopes [233]. They reported that the polysulfone/DMAc dope exhibited extension thinning (i.e., extensional viscosity decreased as extension rate increased) whereas the polyaramide/DMAc solution showed extension thickening (i.e., extensional viscosity increased as extension rate increased). This behavior was attributed to the existence of hydrogen bonding. Their results suggested that polymer dopes with extension thickening behavior may produce hollow fibers with denser morphology, fewer macrovoids and better mechanical properties. Recently, Peng et al. [234] observed similar extension thinning and thickening phenomena for different grades of Torlon® poly(amide-imide) dependent on the degree of hydrogen bonding. They found that a balance between viscoelastic properties, shear and elongational viscosities, and the existence of hydrogen bonding is crucial for the formation of hollow fibers with a defect-free or ultra-thin dense layer.

Since the rheological properties of spin dopes are temperature and moisture sensitive and rheology modifying additives often are added to them, the relationship between shear and elongational viscosities, dope formulation, hydrogen bonding, and temperature must be established for a comprehensive understanding of hollow fiber formation. These relationships will dictate pore size and ultimate separation performance in a given application. This is especially important for high-speed spinning because the effects of elongational viscosity on membrane performance dominate the effects of shear viscosity.

5.3. Green spinning solutions

Ionic liquids, comprising a mixture of cations and anions without an additional solvent, have been considered as a group of environmentally-friendly "green" solvents with unique properties, such as negligible vapor pressure, thermal and chemical stability, recyclability and low flammability [235–238]. Currently, ionic liquids are used primarily as solvents for polymerization and polymer functionalization [235–239]. Since ionic liquids can simplify the dissolution process without creating environmental problems, these green solvents have the potential to replace traditional volatile organic solvents. Xing et al. [240] were the first to report formation of cellulose acetate flat-sheet and hollow fiber membranes using 1-butyl-3- methylimidazolium thiocyanate ([BMIM]SCN) as the solvent via phase inversion in water. They reported the membrane morphology spun from ionic liquids is less porous but macrovoid-free, as opposed to the results for membranes prepared from organic solvents. Since the molecular interactions between polymers and ionic liquids are quite different than those between polymers and conventional organic solvents, membrane scientists must revisit the fundamental science of dope rheology, phase inversion mechanisms, and the effects of spinning parameters when using ionic liquids as solvents to produce useful hollow fibers [241]. It is believed that studies to replace traditional solvents by ionic liquids may establish a new paradigm for membrane formation with the potential to revolutionize the industry.

5.4. Modeling and simulation

Numerous investigators have developed models of the hollow fiber spinning process [7,9,242–254] to correlate or predict the relationships between spinning conditions, membrane structure, and separation performance. Most models are based on previous melt spinning or traditional textile fiber theories summarized by Ziabicki and co-workers [242,243], Pearson [244], and Denn [245]. However, single-layer and multi-layer hollow fiber formation via solution spinning is more complicated than textile fiber fabrication because the former involves two simultaneous phase inversion processes. The majority of this work has focused on the calculation of fiber diameter, dope or bore velocity, temperature and stresses as a function of distance in the draw zone or air-gap region [246–251].

Attempts to predict membrane pore structure as a function of spinning conditions are limited [252–254]. Virtually all efforts assume Newtonian or power-law fluid behavior and neglect the effects of fluid relaxation and radial variations within the fiber cross-section. To advance the current state of the art in simulation, models that account for phase separation on the molecular level and predict three-dimensional, layer-by-layer membrane morphology are needed. The predictions of such models must be validated by comparison with experimental separation measurements.

6. Conclusion and perspectives

This review summarizes the basic principles of polymeric hollow fiber membrane formation via phase inversion. Additionally, major technological advances from the last five decades are identified. Membrane scientists have improved our understanding of macrovoid formation, revealed the importance of dope rheology, developed processes to manufacture dual-layer and mixed matrix membranes, and demonstrated the utility of mathematical modeling. The dual-layer configuration may dominate the production of future hollow fiber membranes.

Breakthroughs in hollow fiber technologies have been made in water reuse, energy production and biofuel separation applications. Many hollow fiber membrane products are available commercially, yet the fundamentals of membrane formation require further investigation. A number of unresolved issues and technical challenges await resolution especially the effects of materials chemistry, hydrogen bonding, and non-solvent additives on rheological characteristics (i.e., strain hardening and thinning), macrovoid formation, pore-size distribution, and selective layer thickness in high-speed spinning processes. A combination of advanced experiments and simulation can help establish the relationships between materials, processing conditions, and membrane performance that will provide the basis for development of the next generation of membranes.

Acknowledgement

The authors would like to thank the Singapore National Research Foundation (NRF) for support from the Competitive Research Programme for the project entitled “Molecular Engineering of Membrane Materials: Research and Technology for Energy Development of Hydrogen, Natural Gas and Syngas” with grant number of R-279-000-261-281.

References

[1] Loeb S, Sourirajan S. Sea water demineralization by means of an osmotic membrane. Adv Chem Ser 1963;38:117–32.
[2] Mahon HI. Permeability separatory apparatus, permeability separatory membrane element, method of making the same and process utilizing the same. US Patent 3,228,876; 1966.
[3] Kesting RE, editor. Synthetic polymeric membranes: a structural perspective. New York: John Wiley & Sons Inc.; 1985.
[4] Lloyd DR, Kinzer KE, Tseng HS. Microporous membrane formation via thermally induced phase separation. I. Solid–liquid phase separation. J Membr Sci 1990;52:239–61.
[5] Ho WSW, Sirkar KK, editors. Membrane handbook. New York: Van Nostrand Reinhold; 1992.
[6] Matsuura T, editor. Synthetic membranes and membrane separation process. Boca Raton, FL, USA: CRC Press; 1994.
[7] Paul DR, Yampol'skii YP, editors. Polymeric gas separation membranes. Boca Raton, FL, USA: CRC Press; 1994.
[8] Koros WJ, Pinnau I. Membrane formation for gas separation process. In: Paul DR, Yampol'skii YP, editors. Polymeric gas separation membranes. Boca Raton, FL, USA: CRC Press; 1994.
[9] Lipscomb GG. The melt hollow fiber spinning process: steady-state behavior, sensitivity and stability. Polym Adv Tech 1994;5:745–58.
[10] Wienk IM, Boom RM, Beerlage MAM, Bulte AMW, Smolders CA, Strathmann H. Recent advances in the formation of phase inversion membranes made from amorphous or semi-crystalline polymers. J Membr Sci 1996;113:361–71.
[11] Chung TS. A review of microporous composite polymeric membrane technology for air-separation. Polym Polym Comp 1996;4:269–83.
[12] Nunes SP, Peinemann KV, editors. Membrane technology in the chemical industry. Weinheim: Wiley-VCH; 2006.
[13] Peng N, Chung TS, Lai JY. The rheology of Torlon® solutions and its role in the formation of ultra-thin defect-free Torlon® hollow fiber membranes for gas separation. J Membr Sci 2009;326:608–17.
[14] Chung TS, Kafchinski ER. The effects of spinning conditions on asymmetric 6FDA/6FDAM polyimide hollow fibers for air separation. J Appl Polym Sci 1997;65:1555–69.
[15] Chung TS. The limitations of using Flory–Huggins equation for the states of solutions during asymmetric hollow fiber formation. J Membr Sci 1997;126:19–34.
[16] Peng N, Chung TS, Wang KY. Macrovoid evolution and critical factors to form macrovoid-free hollow fiber membranes. J Membr Sci 2008;318:363–72.
[17] Mulder MHV. Basic principles of membrane technology. Boston: Kluwer Academic; 1996.
[18] Tompa H. Polymer solutions. London: Butterworths Scientific Publications; 1956.
[19] Strathmann H, Scheible P, Baker RW. A rationale for the preparation of Loeb–Sourirajan-type cellulose acetate membranes. J Appl Polym Sci 1971;15:811–28.
[20] Michaels AS. High flow membrane. US Patent 3,615,024; 1971.
[21] Olabisi O, Robeson LM, Shaw MT. Polymer-polymer miscibility. New York: Academic Press; 1979.
[22] Saxena R, Caneba GT. Studies of spinodal decomposition in a ternary polymer–solvent–nonsolvent system. Polym Eng Sci 2002;42:1019–31.
[23] Fernandes GR, Pinto JC, Nobrega R. Modeling and simulation of the phase-inversion process during membrane formation. J Appl Polym Sci 2001;82:3036–51.
[24] Reuvers AJ, van den Berg JWA, Smolders CA. Formation of membranes by means of immersion precipitation. Part I. A model to describe mass transfer during immersion precipitation. J Membr Sci 1987;34:45–65.
[25] Reuvers AJ, Smolders CA. Formation of membranes by means of immersion precipitation. Part II. The mechanism of formation of membranes prepared from the system cellulose acetate–acetone–water. J Membr Sci 1987;34:67–86.
[26] Tsay CS, McHugh AJ. Mass transfer modeling of asymmetric membrane formation by phase inversion. J Polym Sci B Polym Phys 1990;28:1327–65.
[27] Yilmaz L, McHugh AJ. Modeling of asymmetric membrane formation. II. The effects of surface boundary conditions. J Appl Polym Sci 1988;35:1967–79.
[28] Chung TS, Teoh SK, Hu XD. Formation of ultrathin high-performance polyethersulfone hollow fiber membranes. J Membr Sci 1997;133:161–75.
[29] Chung TS, Teoh SK. Breaking the limitation of composition change during isothermal mass-transfer processes at the spinodal. J Membr Sci 1997;130:141–7.
[30] Shojaie SS, Krantz WB, Greenberg AR. Dense polymer film and membrane formation via dry-cast process. Part I. Model development. J Membr Sci 1994;94:255–80.
[31] Yilmaz L, McHugh AJ. Modeling of asymmetric membrane formation. I. Critique of evaporation models and development of a diffusion equation formalism for the quench period. J Membr Sci 1986;28:287–310.
[32] Sun SP, Wang KY, Rajarathnam D, Hatton TA, Chung TS. Polyamide-imide nanofiltration hollow fiber membranes with elongation-induced nano-pore evolution. AIChE J 2010;56:1481–94.

[33] Pinnau I. Recent advances in the formation of ultrathin polymeric membranes for gas separation. Polym Adv Tech 1994;5:733–44.
[34] van't Hof JA. Wet spinning of asymmetric hollow fibre membranes for gas separation. Ph.D. Dissertation. Univ Twente, Enshede The Netherlands: Univ Twente Publ; 1988.
[35] Cohen C, Tanny GB, Prager S. Diffusion-controlled formation of porous structures in ternary polymer systems. J Polym Sci Polym Phys Ed 1979;17:477–89.
[36] Kim YD, Kim JY, Lee HK, Kim SC. A new modeling of asymmetric membrane formation in rapid mass transfer system. J Membr Sci 2001;190:69–77.
[37] Termonia Y. Monte Carlo diffusion model of polymer coagulation. Phys Rev Lett 1994;72:3678–81.
[38] He X, Chen C, Jiang Z, Su Y. Computer simulation of formation of polymeric ultrafiltration membrane via immersion precipitation. J Membr Sci 2011;371:108–16.
[39] Wang XL, Qian HJ, Chen LJ, Lu ZY, Li ZS. Dissipative particle dynamics simulation on the polymer membrane formation by immersion precipitation. J Membr Sci 2008;311:251–8.
[40] Strathmann H, Kock K, Amar P, Baker RW. The formation mechanism of asymmetric membranes. Desalination 1975;16:179–203.
[41] Pinnau I, Koros WJ. A qualitative skin layer formation mechanism for membranes made by dry/wet phase inversion. J Polym Sci B Polym Phys 1993;31:419–27.
[42] Reuvers AJ, Altena FW, Smolders CA. Demixing and gelation behavior of ternary cellulose acetate solutions. J Polym Sci B Polym Phys 1986;24:793–804.
[43] Kim JY, Kim YD, Kanamori T, Lee HK, Baik KJ, Kim SC. Vitrification phenomena in polysulfone/NMP/water system. J Appl Polym Sci 1999;71:431–8.
[44] van deWitte P, Dijkstra PJ, van den Berg JWA, Feijen J. Phase separation processes in polymer solutions in relation to membrane formation. J Membr Sci 1996;117:1–31.
[45] Young TH, Lin DJ, Gau JJ, Chuang WY, Cheng LP. Morphology of crystalline Nylon-6,10 membranes prepared by the immersion-precipitation process: competition between crystallization and liquid–liquid phase separation. Polymer 1999;40:5011–21.
[46] Matsuyama H, Teramoto M, Nakatani R, Maki T. Membrane formation via phase separation induced by penetration of nonsolvent from vapor phase. II. Membrane morphology. J Appl Polym Sci 1999;74:171–8.
[47] van de Witte P, Esselbrugge H, Dijkstra PJ, van den Berg JWA, Feijen J. Phase transitions during membrane formation of polylactides. I. A morphological study of membranes obtained from the system polylactide–chloroform–methanol. J Membr Sci 1996;113:223–36.
[48] Bulte AMW, Folkers B, Mulder MHV, Smolders CA. Membranes of semicrystalline aliphatic polyamide nylon 4,6: formation by diffusion-induced phase separation. J Appl Polym Sci 1993;50:13–26.
[49] Shih CH, Gryte CC, Cheng LP. Morphology of membranes formed by the isothermal precipitation of polyamide solutions from water/formic acid systems. J Appl Polym Sci 2005;96:944–60.
[50] Young TH, Huang YH, Chen LY. Effect of solvent evaporation on the formation of asymmetric and symmetric membranes with crystallizable EVAL polymer. J Membr Sci 2000;164:111–20.
[51] Doi Y, Matsumura H. Polyvinylidene fluoride porous membrane and a method for producing the same. US Patent 5,022,990; 1991.
[52] Rajabzadeh S, Maruyama T, Sotani T, Matsuyama H. Preparation of PVDF hollow fiber membrane from a ternary polymer/solvent/nonsolvent system via thermally induced phase separation (TIPS) method. Sep Purif Tech 2008;63:415–23.
[53] Young TH, Cheng LP, Lin DJ, Fane L, Chuang WY. Mechanisms of PVDF membrane formation by immersion-precipitation in soft (1-octanol) and harsh (water) nonsolvents. Polymer 1999;40:5315–23.
[54] Buonomenna MG, Macchi P, Davoli M, Drioli E. Poly(vinylidene fluoride) membranes by phase inversion: the role the casting and coagulation conditions play in their morphology, crystalline structure and properties. Eur Polym J 2007;43:1557–72.
[55] Sukitpaneenit P, Chung TS. Molecular elucidation of morphology and mechanical properties of PVDF hollow fiber membranes from aspects of phase inversion, crystallization and rheology. J Membr Sci 2009;340:192–205.
[56] Herbig SR, Cardinal JR, Korsmeyer RW, Smith KL. Asymmetric membrane tablet coating for osmotic drug delivery. J Controlled Release 1995;35:127–36.
[57] Wang DM, Lin FC, Chen LY, Lai JY. Application of TPX membrane to transdermal delivery of nitroglycerin. J Controlled Release 1998;50:187–95.
[58] Smolders CA, Reuvers AJ, Boom RM, Wienk IM. Microstructures in phase-inversion membranes. Part 1. Formation of macrovoids. J Membr Sci 1992;73:259–75.
[59] McHugh AJ, Yilmaz L. The diffusion equation for polymer membrane formation in ternary systems. J Polym Sci A Polym Phys 1985;23:1271–4.
[60] Yao CW, Burford RP, Fane AG, Fell CJD. Effect of coagulation conditions on structure and properties of membranes from aliphatic polyamides. J Membr Sci 1988;38:113–25.
[61] Strathmann H, Kock K. The formation mechanism of phase inversion membranes. Desalination 1977;21:241–55.
[62] Cabasso I, Klein E, Smith JK. Polysulfone hollow fibers. II. Morphology. J Appl Polym Sci 1977;21:165–80.
[63] Levich VG, Krylov VS. Surface-tension-driven phenomena. Annu Rev Fluid Mech 1969;1:293–316.
[64] McKelvey SA, Koros WJ. Phase separation, vitrification, and the manifestation of macrovoids in polymeric asymmetric membranes. J Membr Sci 1996;112:29–39.
[65] Paulsen FG, Shojaie SS, Krantz WB. Effect of evaporation step on macrovoid formation in wet-cast polymeric membranes. J Membr Sci 1994;91:265–82.
[66] Pekny MR, Greenberg AR, Khare V, Zartman J, Krantz WB, Todd P. Macrovoid pore formation in dry-cast cellulose acetate membranes: buoyancy studies. J Membr Sci 2002;205:11–21.
[67] Lai JY, Lin FC, Wu TT, Wang DM. On the formation of macrovoids in PMMA membranes. J Membr Sci 1999;155:31–43.
[68] Wang DM, Lin FC, Wu TT, Lai JY. Formation mechanism of the macrovoids induced by surfactant additives. J Membr Sci 1998;142:191–204.
[69] Won J, Park HC, Kim UY, Kang YS, Yoo SH, Jho JY. The effect of dope solution characteristics on the membrane morphology and gas transport properties: PES/g-BL/NMP system. J Membr Sci 1999;162:247–55.
[70] Fritzsche AK, Arevalo AR, Moore MD, O'Hara C. The surface structure and morphology of polyacrylonitrile membranes by atomic force microscopy. J Membr Sci 1993;81:109–20.
[71] Jiang LY, Chung TS, Li DF, Cao C, Kulprathipanja S. Fabrication of Matrimid/polyethersulfone dual-layer hollow fiber membranes for gas separation. J Membr Sci 2004;240:91–103.
[72] Widjojo N, Chung TS. Thickness and air-gap dependence of macrovoid evolution in phase-inversion asymmetric hollow fiber membranes. Ind Eng Chem Res 2006;45:7618–26.
[73] Teoh MM, Chung TS. Micelle-like macrovoids in mixed matrix PVDF-PTFE hollow fiber membranes. J Membr Sci 2009;338:5–10.
[74] Kesting RE, Fritzsche AK, Murphy MK, Handermann AC, Cruse CA, Malon RF. Process for forming asymmetric gas separation membranes having graded density skins. US Patent 4,871,494; 1989.
[75] Liu Y, Koops GH, Strathmann H. Characterization of morphology controlled polyethersulfone hollow fiber membranes by the addition of polyethylene glycol to the dope and bore fluid solution. J Membr Sci 2003;223:187–99.
[76] Li DF, Chung TS, Wang R. Morphological aspects and structure control of dual-layer asymmetric hollow fiber membranes formed by a simultaneous co-extrusion approach. J Membr Sci 2004;243:155–75.
[77] Lin KY, Wang DM, Lai JY. Nonsolvent-Induced gelation and its effect on membrane morphology. Macromolecules 2002;35:6697–706.
[78] Tsai HA, Li LD, Lee KR, Wang YC, Li CL, Huang J, Lai JY. Effect of surfactant addition on the morphology and pervaporation performance of asymmetric polysulfone membranes. J Membr Sci 2000;176:97–103.
[79] Wang KY, Li DF, Chung TS, Chen SB. The observation of elongation dependent macrovoid evolution in single- and dual-layer asymmetric hollow fiber membranes. Chem Eng Sci 2004;59:4657–60.
[80] Cao C, Chung TS, Chen SB, Dong Z. The study of elongation and shear rates in spinning process and its effect on gas separation performance of poly (ethersulfone)(PES) hollow fiber membranes. Chem Eng Sci 2004;59:1053–62.
[81] Xiao YC, Wang KY, Chung TS, Tan JN. Evolution of nano-particle distribution during the fabrication of mixed matrix TiO_2–polyimide hollow fiber membranes. Chem Eng Sci 2006;61:6228–33.
[82] Vogrin N, Stropnik C, Musil V, Brumen M. The wet phase separation: the effect of cast solution thickness on the appearance of macrovoids in the membrane forming ternary cellulose acetate/acetone/water system. J Membr Sci 2002;207:139–41.
[83] Li DF, Chung TS, Ren JZ, Wang R. Thickness dependence of macrovoid evolution in wet phase-inversion asymmetric membranes. Ind Eng Chem Res 2004;43:1553–6.

[84] Husain S, Koros WJ. Macrovoids in hybrid organic/inorganic hollow fiber membranes. Ind Eng Chem Res 2009;48:2372–9.
[85] Tsai HA, Kuo CY, Lin JH, Wang DM, Deratani A, Pochat-Bohatier C, Lee KR, Lai JY. Morphology control of polysulfone hollow fiber membranes via water vapor induced phase separation. J Membr Sci 2006;278:390–400.
[86] Yin J, Coutris N, Huang Y. Role of Marangoni instability in fabrication of axially and internally grooved hollow fiber membranes. Langmuir 2010;26:16991–9.
[87] Roesink HDW. The influence of spinning conditions on the morphology of microporous capillary membranes. Ph.D. Dissertation. Univ Twente, Enshede The Netherlands: Univ Twente Publ; 1989 [Chapter 3].
[88] Yan JS. Polysulfone hollow fiber membrane-effect of internal coagulant on membrane morphology. M.E. Dissertation, National University of Singapore. Singapore:National University of Singapore; 1996.
[89] McKelvey SA, Clausi DT, Koros WJ. A guide to establishing hollow fiber macroscopic properties for membrane application. J Membr Sci 1997;124:223–32.
[90] Pereira CC, Nobrega R, Borges CP. Spinning process variables and polymer solution effects in the die swell phenomenon during hollow fiber membrane formation. Brazil J Chem Eng 2000;17:4–7.
[91] Kang JS, Lee YM. Effects of molecular weight of polyvinylpyrrolidone on precipitation kinetics during the formation of asymmetric polyacrylonitrile membrane. J Appl Polym Sci 2002;85:57–68.
[92] Santoso YE, Chung TS, Wang KY, Weber M. The investigation of irregular inner skin morphology of hollow fiber membranes at high-speed spinning and the solutions to overcome it. J Membr Sci 2006;282:383–92.
[93] Bonyadi S, Chung TS, Krantz WB. Investigation of corrugation phenomenon in the inner contour of hollow fibers during the non-solvent induced phase-separation process. J Membr Sci 2007;299:200–10.
[94] Greenhill AG. The elastic curve under uniform normal pressure. Math Ann 1899;52:465–500.
[95] Shi L, Wang R, Cao Y, Feng C, Liang DT, Tay JH. Fabrication of poly(vinylidene fluoride-*co*-hexafluropropylene) (PVDF-HFP) asymmetric microporous hollow fiber membranes. J Membr Sci 2007;305:215–25.
[96] Shi L, Wang R, Cao Y. Effect of the rheology of poly(vinylidene fluoride-co-hexafluropropylene)(PVDF–HFP) dope solutions on the formation of microporous hollow fibers used as membrane contactors. J Membr Sci 2009;344:112–22.
[97] Zhang X, Wen Y, Yang Y, Liu L. Effect of air-gap distance on the formation and characterization of hollow polyacrylonitrile (PAN) nascent fibers. J Macromol Sci Part B 2008;47:1039–49.
[98] Henis JMS, Tripodi MK. Composite hollow fiber membranes for gas separation: the resistance model approach. J Membr Sci 1981;8:233–46.
[99] Pinnau I, Koros WJ. Gas-permeation properties of asymmetric polycarbonate, polyestercarbonate, and fluorinated polyimide membranes prepared by the generalized dry-wet phase inversion process. J Appl Polym Sci 1992;46:1195–204.
[100] Clausi DT, Koros WJ. Formation of defect-free polyimide hollow fiber membranes for gas separations. J Membr Sci 2000;167:79–89.
[101] Kosuri MR, Koros WJ. Defect-free asymmetric hollow fiber membranes from Torlon®, a polyamide–imide polymer, for high-pressure CO_2 separations. J Membr Sci 2008;320:65–72.
[102] Peng N, Chung TS. The effects of spinneret dimension and hollow fiber dimension on gas separation performance of ultrathin defect-free Torlon® hollow fiber membranes. J Membr Sci 2008;310:455–65.
[103] Pinnau I, Wijmans JG, Blume I, Kuroda T, Peinemann KV. Gas permeation through composite membranes. J Membr Sci 1988;37:81–8.
[104] Kimmerle K, Hofmann T, Strathmann H. Analysis of gas permeation through composite membranes. J Membr Sci 1991;61:1–17.
[105] Gudernatsch W, Menzel Th, Strathmann H. Influence of composite membrane structure on pervaporation. J Membr Sci 1991;61:19–30.
[106] Chung TS, Kafchinski ER, Foley P, Kohn RS, Straff RS. Fabrication of composite hollow fibers for air separation. J Appl Polym Sci 1994;53:701–8.
[107] Chung TS, Shieh JJ, Lau WYW, Srinivasan MP, Paul DR. Fabrication of multi-layer microporous composite membranes for gas separation. J Membr Sci 1999;152:211–25.
[108] Liu Y, Feng X, Lawless D. Separation of gasoline vapor from nitrogen by hollow fiber composite membranes for VOC emission control. J Membr Sci 2006;271:114–24.
[109] Du R, Chakma A, Feng X. Interfacially formed poly(*N*,*N*-dimethylaminoethyl methacrylate)/polysulfone composite membranes for CO_2/N_2 separation. J Membr Sci 2007;290:19–28.
[110] Kneifel K, Peinemann K-V. Preparation of hollow fiber membranes from polyetherimide for gas separation. J Membr Sci 1992;65:295–307.
[111] Kuzumoto E, Nitta K. Manufacture of permselective hollow membranes. JP 01015104, 1989.
[112] Ekiner OM, Hayes RA, Manos P. Novel multicomponent fluid separation membranes. US Patent 5,085,676; 1992.
[113] Nago S, Mizutani Y. Microporous polypropylene hollow fibers with double layers. J Membr Sci 1996;116:1–7.
[114] Suzuki H, Tanaka K, Kita H, Okamoto K, Hoshino H, Yoshinaga T, Kusuki Y. Preparation of composite hollow fiber membranes of poly (ethylene oxide)-containing polyimide and their CO_2/N_2 separation properties. J Membr Sci 1998;146:31–7.
[115] Yang S, Teo WK, Li K. Formation of annular hollow fibers for immobilization of yeast in annular passages. J Membr Sci 2001;184:107–15.
[116] He T, Mulder MHV, Strathmann H, Wessling M. Preparation of composite hollow fiber membranes: co-extrusion of hydrophilic coating onto porous hydrophobic support structures. J Membr Sci 2002;207:143–56.
[117] Pereira CC, Nobrega R, Peinemann KV, Borges CP. Hollow fiber membranes obtained by simultaneous spinning of two polymer solutions: a morphological study. J Membr Sci 2003;226:35–50.
[118] Li Y, Cao C, Chung TS, Pramoda KP. Fabrication of dual-layer polyethersulfone (PES) hollow fiber membranes with an ultrathin dense selective layer for gas separation. J Membr Sci 2004;245:53–60.
[119] Peng N, Chung TS, Chng ML, Aw W. Evolution of ultra-thin dense-selective layer from single-layer to dual-layer hollow fibers using novel Extem® polyetherimide for gas separation. J Membr Sci 2010;360:48–57.
[120] Jiang LY, Chen H, Jean YC, Chung TS. Ultrathin polymeric interpenetration network with separation performance approaching ceramic membranes for biofuel. AIChE J 2009;55:75–86.
[121] Kopec KK, Dutczak SM, Wessling M, Stamatialis DF. Chemistry in a spinneret—on the interplay of crosslinking and phase inversion during spinning of novel hollow fiber membranes. J Membr Sci 2011;369:308–18.
[122] Cao C, Chung TS, Liu Y, Wang R, Pramoda KP. Chemical cross-linking modification of 6FDA-2,6-DAT hollow fiber membranes for natural gas separation. J Membr Sci 2003;216:257–68.
[123] Visser T, Koops GH, Wessling M. On the subtle balance between competitive sorption and plasticization effects in asymmetric hollow fiber gas separation membranes. J Membr Sci 2005;252:265–77.
[124] Ismail AF, Yaacob N. Performance of treated and untreated asymmetric polysulfone hollow fiber membrane in series and cascade module configurations for CO_2/CH_4 gas separation system. J Membr Sci 2006;275:151–65.
[125] Liu L, Wang R, Chung TS. Chemically cross-linking modification of polyimide membranes for gas separation. J Membr Sci 2001;189:231–9.
[126] Peter J, Peinemann KV. Multilayer composite membranes for gas separation based on crosslinked PTMSP gutter layer and partially crosslinked Matrimid® 5218 selective layer. J Membr Sci 2009;340:62–72.
[127] Koros WJ, Wallace D, Wind JD, Miller SJ, Staudt-Bickel C, Vu DQ. Crosslinked and crosslinkable hollow fiber mixed matrix membrane and method of making same. US Patent 6,755,900; 2004.
[128] Park HB, Jung CH, Lee YM, Hill AJ, Pas SJ, Mudie ST, Wagner EV, Freeman BD, Cookson DJ. Polymers with cavities tuned for fast selective transport of small molecules and ions. Science 2007;318:254–8.
[129] Park HB, Han SH, Jung JH, Lee YM, Hill AJ. Thermally rearranged (TR) polymer membranes for CO_2 separation. J Membr Sci 2010;359:11–24.
[130] Budd PM, Elabas ES, Ghanem BS, Makhseed S, McKeown NB, Msayib KJ, Tattershall CE, Wang D. Solution-processed, organophilic membrane derived from a polymer of intrinsic microporosity. Adv Mater 2004;16:456–9.
[131] Du N, Park HB, Robertson GP, Dal-Cin MM, Visser T, Scoles L, Guiver MD. Polymer nanosieve membranes for CO_2-capture applications. Nat Mater 2011;10:372–5.
[132] Welton T. Room-temperature ionic liquids. Solvents for synthesis and catalysis. Chem Rev 1999;99:2071–83.
[133] Blanchard LA, Hancu D, Beckman EJ, Brennecke JF. Green processing using ionic liquids and CO_2. Nature 1999;399:28–9.

[134] Li P, Pramoda KP, Chung TS. CO_2 separation from flue gas using polyvinyl-(room temperature ionic liquid)—room temperature ionic liquid composite membranes. Ind Eng Chem Res 2011;50:9344–53.
[135] Perez EV, Balkus Jr KJ, Ferraris JP, Musselman IH. Mixed-matrix membranes containing MOF-5 for gas separations. J Membr Sci 2009;328:165–73.
[136] Yang T, Xiao Y, Chung TS. Poly-/metal-benzimidazole nanocomposite membranes for hydrogen purification. Energy Environ Sci 2011;4:4171–80.
[137] Lin H, Van Wagner E, Freeman BD, Toy LG, Gupta RP. Plasticization-enhanced hydrogen purification using polymeric membranes. Science 2006;311:639–42.
[138] Car A, Stropnik C, Yave W, Peinemann KV. Tailor-made polymeric membranes based on segmented block copolymers for CO_2 separation. Adv Funct Mater 2008;18:2815–23.
[139] Lau CH, Liu S, Paul DR, Xia J, Jean YC, Chen H, Shao L, Chung TS. Silica nanohybrid membranes with high CO_2 affinity for green hydrogen purification. Adv Eng Mater 2011;1:634–42.
[140] Xia J, Liu S, Lau CH, Chung TS. Liquid like poly(ethylene glycol) supported in the organicinorganic matrix for CO_2 removal. Macromolecules 2011;44:5268–80.
[141] Chen HZ, Xiao YC, Chung TS. Multi-layer composite hollow fiber membranes derived from poly(ethylene glycol) (PEG) containing hybrid materials for CO_2/N_2 separation. J Membr Sci 2011;381:211–20.
[142] Kulprathipanja S, Neuzil RW, Li NN. Separation of fluids by means of mixed matrix membranes. US Patent 4,740,219; 1988.
[143] Zimmerman CM, Singh A, Koros WJ. Tailoring mixed matrix composite membranes for gas separations. J Membr Sci 1997;137:145–54.
[144] Merkel TC, Freeman BD, Spontak RJ, He Z, Pinnau I, Meakin P, Hill AJ. Ultrapermeable, reverse-selective nanocomposite membranes. Science 2002;296:519–22.
[145] Chung TS, Jiang LY, Li Y, Kulprathipanja S. Mixed matrix membranes (MMMs) comprising organic polymers with dispersed inorganic fillers for gas separation. Prog Polym Sci 2007;32:483–507.
[146] Widjojo N, Li Y, Jiang LY, Chung TS. Recent progress and challenges on mixed matrix membranes in both material and configuration aspects for gas separation. Advanced materials for membrane preparation (E-book). Oak Park Illinois: Bentham Science Publishers; in press.
[147] Robeson LM. Correlation of separation factor versus permeability for polymeric membranes. J Membr Sci 1991;62:165–85.
[148] Jiang LY, Chung TS, Kulprathipanja S. An investigation to revitalize the separation performance of hollow fibers with a thin mixed matrix composite skin for gas separation. J Membr Sci 2006;276:113–25.
[149] Miller SJ, Munson CL, Kulkarni SS, Hasse DJ. Purification of *p*-xylene using composite mixed matrix membranes. US Patent 6,500,233; 2002.
[150] Ekiner OM, Kulkarni SS. Process for making hollow fiber mixed matrix membranes. US Patent 6,663,805; 2003.
[151] Koros WJ, Vu DQ, Mahajan R, Miller SJ. Gas separations using mixed matrix membranes. US Patent 6,503,295; 2003.
[152] Li Y, Chung TS, Huang Z, Kulprathipanja S. Dual-layer polyethersulfone (PES)/BTDA-TDI/MDI co-polyimide (P84) hollow fiber membranes with a submicron PES–zeolite beta mixed matrix dense-selective layer for gas separation. J Membr Sci 2006;277:28–37.
[153] Husain S, Koros WJ. Mixed matrix hollow fiber membranes made with modified HSSZ-13 zeolite in polyetherimide polymer matrix for gas separation. J Membr Sci 2007;288:195–207.
[154] Shu S, Husain S, Koros WJ. Formation of nanostructured zeolite particle surfaces via a halide/grignard route. Chem Mater 2007;19:4000–6.
[155] Shu S, Husain S, Koros WJ. A general strategy for adhesion enhancement in polymeric composites by formation of nanostructured particle surfaces. J Phys Chem C 2007;111:652–7.
[156] Widjojo N, Chung TS, Kulprathipanja S. The fabrication of hollow fiber membranes with double-layer mixed-matrix materials for gas separation. J Membr Sci 2008;325:326–35.
[157] Li Y, Krantz WB, Chung TS. A novel primer to prevent nanoparticle agglomeration in mixed matrix membranes. AIChE J 2007;53:2470–5.
[158] Li Y, Chung TS, Kulprathipanja S. Novel Ag^+-zeolite/polymer mixed matrix membranes with a high CO_2/CH_4 selectivity. AIChE J 2007;53:610–6.
[159] Feng XS, Huang RYM. Preparation and performance of asymmetric polyetherimide membranes for isopropanol dehydration by pervaporation. J Membr Sci 1996;109:165–72.
[160] Wei YM, Xu ZL, Qusay FA, Wu K. Polyvinyl alcohol/polysulfone (PVA/PSf) hollow fiber composite membranes for pervaporation separation of ethanol/water solution. J Appl Polym Sci 2005;98:247–54.
[161] Dong YQ, Zhang L, Shen JN, Song MY, Chen HL. Preparation of poly(vinyl alcohol)-sodium alginate hollow fiber composite membranes and pervaporation dehydration characterization of aqueous alcohol mixtures. Desalination 2006;193:202–10.
[162] Xu ZK, Dai QW, Liu ZM, Kou RQ, Xu YY. Microporous polypropylene hollow fiber membranes. Part II. Pervaporation separation of water/ethanol mixtures by the poly(acrylic acid) grafted membranes. J Membr Sci 2003;214:71–81.
[163] Tsai HA, Chen HC, Chou WL, Lee KR, Yang MC, Lai JY. Pervaporation of water/alcohol mixtures through chitosan/cellulose acetate composite hollow fiber membranes. J Appl Polym Sci 2004;94:1562–8.
[164] Jiang LY, Chung TS, Rajagopalan R. Dehydration of alcohols by pervaporation through polyimide Matrimid® asymmetric hollow fibers with various modifications. Chem Eng Sci 2008;63:204–16.
[165] Wang Y, Gruender M, Chung TS. Pervaporation dehydration of ethylene glycol through polybenzimidazole (PBI)-based membranes. 1. Membrane fabrication. J Membr Sci 2010;363:149–59.
[166] Kung G, Jiang LY, Wang Y, Chung TS. Asymmetric hollow fibers by polyimide and polybenzimidazole blends for toluene/iso-octane separation. J Membr Sci 2010;360:303–14.
[167] Chapman PD, Oliveira T, Livingston AG, Li K. Membranes for the dehydration of solvents by pervaporation. J Membr Sci 2008;318:5–37.
[168] Feng X, Huang RYM. Liquid separation by membrane pervaporation: a review. Ind Chem Eng Res 1997;36:1048–66.
[169] Song M, Shen J, Chen H. Sodium alginate and polyvinyl alcohol hollow fiber composite membrane for dehydration of isopropanol. J Petrochem Technol 2004;33:216–9.
[170] Lang WZ, Tong W, Xu ZL. Preparation of PFSA-PVA/PSf hollow fiber membrane for IPA/H2O pervaporation process. J Appl Polym Sci 2008;108:370–9.
[171] Shen JN, Wu LG, Qui JH, Gao CJ. Pervaporation separation of water/isopropanol mixtures through crosslinked carboxymethyl chitosan/polysulfone hollow fiber composite membrane. J Appl Polym Sci 2007;103:1959–65.
[172] Tsai HA, Chen WH, Kuo CY, Lee KR, Lai JY. Study on the pervaporation performance and long term stability of aqueous isopropanol solution through chitosan/polyacrylonitrile hollow fiber membrane. J Membr Sci 2008;309:146–55.
[173] Tsai HA, Ciou YS, Hu CC, Lee KR, Yu DG, Lai JY. Heat-treatment effect on the morphology and pervaporation performances of asymmetric PAN hollow fiber membranes. J Membr Sci 2005;255:33–47.
[174] Qiu W, Kosuri M, Zhou F, Koros WJ. Dehydration of ethanol–water mixtures using asymmetric hollow fiber membranes from commercial polyimides. J Membr Sci 2009;327:96–103.
[175] Wang Y, Goh SH, Chung TS, Peng N. Polyamide-imide/polyetherimide dual-layer hollow fiber membranes for pervaporation dehydration of C_1–C_4 alcohols. J Membr Sci 2009;326:222–33.
[176] Jiang LY, Wang Y, Chung TS, Qiao XY, Lai JY. Polyimides for pervaporation membranes and biofuels separation. Prog Polym Sci 2009;34:1135–60.
[177] Liu RX, Qiao XY, Chung TS. The development of high performance P84 co-polyimide hollow fibers for pervaporation dehydration of isopropanol. Chem Eng Sci 2005;60:6674–86.
[178] Shi GM, Wang Y, Chung TS. Dual-layer PBI/P84 hollow fibers for pervaporation dehydration of acetone. AIChE J in press; doi: 10.1002/aic.12625.
[179] Le NL, Wang Y, Chung TS. Pebax/POSS mixed matrix membranes for ethanol recovery from aqueous solutions via pervaporation. J Membr Sci 2011;379:174–83.
[180] Wang Y, Chung TS, Wang H. Polyamide-imide membranes with surface immobilized cyclodextrin for butanol isomer separation via pervaporation. AIChE J 2011;57:1470–84.
[181] Guo J, Zhang G, Wu W, Ji S, Qin Z, Liu Z. Dynamically formed inner skin hollow fiber polydimethylsiloxane/polysulfone composite membrane for alcohol permselective pervaporation. Chem Eng J 2010;158:558–65.
[182] Sukitpaneenit P, Chung TS, Jiang LY. Modified pore-flow model for pervaporation mass transport in PVDF hollow fiber membranes for ethanol–water separation. J Membr Sci 2010;362:393–406.

[183] Sukitpaneenit P, Chung TS. Molecular design of the morphology and pore size of PVDF hollow fiber membranes for ethanol–water separation employing the modified pore-flow concept. J Membr Sci 2011;374:67–82.
[184] Teoh MM, Wang KY, Bonyadi S, Yang Q, Chung TS. Emerging membrane technologies developed in NUS for water reuse and desalination applications: membrane distillation and forward osmosis. Membr Water Treat 2011;2:1–24.
[185] Chung TS, Zhang S, Wang KY, Su JC, Ling MM. Forward osmosis processes: yesterday, today and tomorrow. Desalination 2012;287:78–81.
[186] Paul DR. Reformulation of the solution–diffusion theory of reverse osmosis. J Membr Sci 2004;241:371–86.
[187] Wijrnans JG, Baker RW. The solution–diffusion model: a review. J Membr Sci 1995;107:1–21.
[188] Wang KY, Chung TS, Qin JJ. Polybenzimidazole (PBI) nanofiltration hollow fiber membranes applied in forward osmosis process. J Membr Sci 2007;300:6–12.
[189] Yang Q, Wang KY, Chung TS. Dual-layer hollow fibers with enhanced flux as novel forward osmosis membranes for water production. Environ Sci Technol 2009;43:2800–5.
[190] Wang KY, Yang Q, Chung TS, Rajagopalan R. Enhanced forward osmosis from chemically modified polybenzimidazole (PBI) nanofiltration hollow fiber membranes with a thin wall. Chem Eng Sci 2009;64:1577–84.
[191] Su JC, Yang Q, Teo JF, Chung TS. Cellulose acetate nanofiltration hollow fiber membranes for forward osmosis processes. J Membr Sci 2010;355:36–44.
[192] Su JC, Zhang S, Chen H, Chen H, Jean YC, Chung TS. Effects of annealing on the microstructure and performance of cellulose acetate membranes for pressure-retarded osmosis processes. J Membr Sci 2010;364:344–53.
[193] Cadotte JE, Rozelle LT. In situ-formed condensation of polymers for reverse osmosis membranes. OSW PB-Report No. 927; 1972.
[194] Cadotte JE. Reverse osmosis membrane. US Patent 4,039,440; 1977.
[195] Verissimo S, Peinemann KV, Bordado J. Thin-film composite hollow fibre membranes: an optimized manufacturing method. J Membr Sci 2005;264:48–55.
[196] Ghosh AK, Jeong BH, Huang XF, Hoek EMV. Impacts of reaction and curing conditions on polyamide composite reverse osmosis membrane properties. J Membr Sci 2008;311:34–45.
[197] McCutcheon JR, Elimelech M. Influence of membrane support layer hydrophobicity on water flux in osmotically driven membrane processes. J Membr Sci 2008;318:458–66.
[198] Yip NY, Tiraferri A, Phillip WA, Schiffman JD, Elimelech M. High performance thin-film composite forward osmosis. Environ Sci Technol 2010;44:3812–8.
[199] Wang R, Shi L, Tang CY, Chou S, Qiu CQ, Fane AG. Characterization of novel forward osmosis hollow fiber membranes. J Membr Sci 2010;355:158–67.
[200] Wang KY, Chung TS, Amy G. Developing thin-film-composite forward osmosis membranes based on the PES/SPSf substrate through interfacial polymerization. AIChE J 2012;58:770–81.
[201] Widjojo N, Chung TS, Weber M, Maletzko C, Warzelhan V. The role of sulphonated polymer and macrovoid-free structure in the support layer for thin-film composite (TFC) forward osmosis (FO) membranes. J Membr Sci 2011;383:214–23.
[202] Lagana F, Barbieri G, Drioli E. Direct contact membrane distillation: modeling and concentration experiments. J Membr Sci 2000;166:1–11.
[203] El-bourawi MS, Ding Z, Ma R, Khayet M. A frame work for better understanding membrane distillation separation process. J Membr Sci 2006;285:4–29.
[204] Al-Obaidani S, Curcio E, Macedonio F, Profio GD, Al-Hinai H, Drioli E. Potential of membrane distillation in seawater desalination: thermal efficiency, sensitivity study and cost estimation. J Membr Sci 2008;323:85–98.
[205] Bonyadi S, Chung TS. Highly porous and macrovoid-free PVDF hollow fiber membranes for membrane distillation by solvent-dope solution co-extrusion approach. J Membr Sci 2009;331: 66–74.
[206] Curcio E, Drioli E. Membrane distillation and related operation—a review. Sep Purif Rev 2005;34:35–86.
[207] Gryta M, Tomaszewska M. Heat transport in the membrane distillation process. J Membr Sci 1998;144:211–22.
[208] Li B, Sirkar KK. Novel membrane and device for direct contact membrane distillation-based desalination process. Ind Eng Chem Res 2004;43:5300–9.
[209] Bonyadi S, Chung TS. Flux enhancement in membrane distillation by fabrication of dual layer hydrophilic–hydrophobic hollow fiber membranes. J Membr Sci 2007;306:134–46.
[210] Teoh MM, Chung TS. Membrane distillation with hydrophobic macrovoid-free PVDF–PTFE hollow fiber membranes. Sep Purif Tech 2009;66:229–36.
[211] Wang KY, Foo SW, Chung TS. Mixed matrix PVDF hollow fiber membranes with nano-scale pores for desalination through direct contact membrane distillation. Ind Eng Chem Res 2009;48:4474–83.
[212] Bonyadi S, Chung TS, Rajagopalan R. A novel approach to fabricate highly concentric, macrovoid-free and highly permeable PVDF hollow fiber membranes with thin wall for membrane distillation. AIChE J 2009;55:828–33.
[213] Khayet M. Membranes and theoretical modeling of membrane distillation: a review. Adv Colloid Interface Sci 2011;164:56–88.
[214] Khayet M, Cojocaru C, Essalhi M, Garcia-Payo MC, Arribas P, Garcia-Fernandez L. Hollow fiber spinning experimental design and analysis of defects for fabrication of optimized membranes for membrane distillation. Desalination in press; doi:10.1016/j.desal.2011.06.025.
[215] Wang D, Li K, Teo WK. Porous PVDF asymmetric hollow fiber membranes prepared with the use of small molecular additives. J Membr Sci 2000;178:13–23.
[216] Yeow ML, Liu Y, Li K. Preparation of porous PVDF hollow fiber membrane via a phase inversion method using lithium perchlorate ($LiClO_4$) as an additive. J Membr Sci 2005;258:16–22.
[217] Wang KY, Matsuura T, Chung TS, Guo WF. The effects of flow angle and shear rate within the spinneret on the separation performance of poly(ethersulfone) (PES) ultrafiltration hollow fiber membranes. J Membr Sci 2004;240:67–79.
[218] Nijdam W, de Jong J, van Rijn CJM, Visser T, Versteeg L, Kapantaidakis G, Koops GH, Wessling M. High performance micro-engineered hollow fiber membranes by smart spinneret design. J Membr Sci 2005;256:209–15.
[219] Widjojo N, Chung TS, Krantz WB. A morphological and structural study of Ultem/P84 copolyimide dual-layer hollow fiber membranes with delamination-free morphology. J Membr Sci 2007;294:132–46.
[220] Yang Q, Chung TS, Weber M, Wollny K. Rheological investigations of linear and hyperbranched polyethersulfone towards their as-spun phase inversion membranes differences. Polymer 2009;50:524–33.
[221] Widjojo N, Chung TS, Arifin DY, Weber M, Warzelhan V. Elimination of die swell and instability in hollow fiber spinning process of hyperbranched polyethersulfone (HPES) via novel spinneret designs and precise spinning conditions. Chem Eng J 2010;163:143–53.
[222] Çulfaz PZ, Wessling M, Lammertink RGH. Hollow fiber ultrafiltration membranes with microstructured inner skin. J Membr Sci 2011;369:221–7.
[223] Toshiji O. Hollow tape-shaped membrane and its production JP 11090192; 1979.
[224] Hallmark B, Gadala-Maria F, Mackley MR. The melt processing of polymer microcapillary film (MCF). Non-Newtonian Fluid Mech 2005;128:83–98.
[225] Peng N, Teoh MM, Chung TS, Koo LL. Novel rectangular membranes with multiple hollow holes for ultrafiltration. J Membr Sci 2011;372:20–8.
[226] Anonymous SevenBore® UF membrane. Innovative Membrane Technologies B.V. http://www.imtmembranes.nl/technical.html; 2010 [accessed January 2012].
[227] Han CD. Rheology in polymer processing. New York: Academic Press, Inc.; 1976.
[228] Qin JJ, Wang R, Chung TS. Investigation of shear stress effect within a spinneret on flux, separation and thermomechanical properties of hollow fiber ultrafiltration membranes. J Membr Sci 2000;175:197–213.
[229] Chung TS, Teoh SK, Lau WWY, Srinivasan MP. Effect of shear stress within the spinneret on hollow fiber membrane morphology and separation performance. Ind Eng Chem Res 1998;37:3930–8.
[230] East GC, Mclntyre JE, Rogers V, Senn SC. Production of porous hollow polysulfone fibers for gas separation. In: Proceedings of the 4th BOC Priestly Conference. London: Royal Society of Chemistry; 1986 [Special Publication No. 62].
[231] Shilton SJ, Bell G, Ferguson J. The rheology of fiber spinning and the properties of hollow fiber membranes for gas separation. Polymer 1994;35:5327–35.
[232] Ren JZ, Chung TS, Li DF, Wang R, Liu Y. Development of asymmetric 6FDA-2,6 DAT hollow fiber membranes for CO_2/CH_4 separation—1. The influence of dope composition and rheology on

membrane morphology and separation performance. J Membr Sci 2002;207:227–40.
[233] Ekiner OM, Vassilatos G. Polyaramide hollow fibers for hydrogen/methane separation-spinning and properties. J Membr Sci 1990;53:259–73.
[234] Peng N, Chung TS, Kwok YL. The role of additives on dope rheology and membrane formation of defect-free Torlon® hollow fibers for gas separation. J Membr Sci 2009;343:62–72.
[235] Earle MJ, Seddon KR. Ionic liquids. Green solvents for the future. Pure Appl Chem 2000;72:1391–8.
[236] Rogers RD, Seddon KR. Ionic liquids–solvents of the future? Science 2003;302:792–3.
[237] Seoud OA, Koschella A, Fidale LC, Dorn S, Heinze T. Applications of ionic liquids in carbohydrate chemistry: a window of opportunities. Biomacromolecules 2007;8:2629–47.
[238] Ueki T, Watanabe M. Macromolecules in ionic liquids: progress, challenges and opportunities. Macromolecules 2008;41:3739–49.
[239] Wong H, Han S, Livingston AG. The effect of ionic liquids on product yield and catalyst stability. Chem Eng Sci 2006;61:1338–41.
[240] Xing DY, Peng N, Chung TS. Formation for cellulose acetate membranes via phase inversion using ionic liquid, [BMIM]SCN, as the solvent via phase inversion. Ind Eng Chem Res 2010;49:8761–9.
[241] Xing DY, Peng N, Chung TS. Investigation of unique interactions between cellulose acetate and ionic liquid, [EMIM]SCN, and their influences on hollow fiber ultrafiltration membranes. J Membr Sci 2011;380:87–97.
[242] Ziabicki A. Fundamentals of fiber formation. London: Wiley; 1976.
[243] Ziabicki A, Kawai H. High speed fiber spinning, science and engineering aspects. Melbourne, FL, USA: Krieger; 1991.
[244] Pearson JRA. Mechanical principles of polymer melt processing. London: Pergamon; 1966.
[245] Denn MM. Polymer melt processing: foundations in fluid mechanics and heat transfer. Cambridge, UK: Cambridge Univ. Press; 2008.
[246] Freeman BD, Denn MM, Keunings R, Molau GE, Ramos J. Profile development in drawn hollow tubes. J Polym Eng 1986;6:171–86.
[247] Radovanovic P, Thiel SW, Hwang ST. Formation of asymmetric polysulfone membranes by immersion precipitation. Part I. Modelling mass transport during gelation. J Membr Sci 1992;65:213–29.
[248] Chung TS, Xu ZL, Lin WH. Fundamental understanding of the effect of air-gap distance on the fabrication of hollow fiber membranes. J Appl Polym Sci 1999;72:379–95.
[249] Oh TH, Lee MS, Kim SY, Shim HJ. Studies on melt-spinning process of hollow fibers. J Appl Polym Sci 1998;68:1209–17.
[250] Simon V. Analysis of fiber spinning during air-gap wet spinning. AIChE J 1995;41:1281–94.
[251] Su Y, Lipscomb GG, Balasubramanian H, Lloyd DR. Observations of recirculation in the bore fluid during hollow fiber spinning. AIChE J 2006;52:2072–8.
[252] Aroon MA, Ismail AF, Montazer-Rahmati MM, Matsuura T. A mathematical analysis of hollow fiber spinning: bore and dope velocity profiles in the air-gap. J Membr Sci 2010;348:13–20.
[253] Matsuyama H, Yuasa M, Kitamura Y, Teramoto M, Lloyd DR. Structure control of anistropic and asymmetric polypropylene membranes prepared by thermally induced phase separation. J Membr Sci 2000;179:91–100.
[254] Balasubramanian-Rauckhorst HA, Lloyd DR, Lipscomb GG. Predicting extent of anisotropy in anisotropic hollow fiber membrane formation. J Membr Sci 2009;339:250–60.